STUDY OF LASER INDUCED COOLING IN LOW PRESSURE GASES

By

DINESH KUMAR JAIN

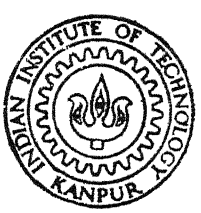

DEPARTMENT OF MECHANICAL ENGINEERING

INDIAN INSTITUTE OF TECHNOLOGY, KANPUR

APRIL, 1984

STUDY OF LASER INDUCED COOLING IN LOW PRESSURE GASES

A Thesis Submitted
In Partial Fulfilment of the Requirements
for the Degree of
MASTER OF TECHNOLOGY

By
DINESH KUMAR JAIN

to the
DEPARTMENT OF MECHANICAL ENGINEERING
INDIAN INSTITUTE OF TECHNOLOGY, KANPUR
APRIL, 1984

CERTIFICATE

This is to certify that the thesis entitled 'STUDY OF LASER INDUCED COOLING IN LOW PRESSURE GASES' by DINESH KUMAR JAIN is a record of work carried out under our supervision and has not been submitted elsewhere for a degree.

(M.S. Kalra)
Assistant Professor
Department of Mech.Engg.
I.I.T. Kanpur.

(J.S. Goela)
Assistant Professor
Department of Mech.Engg.
I.I.T. Kanpur.

ACKNOWLEDGEMENTS

It is with immense pleasure and great respect that I express my deep sense of gratitude to Dr. M.S. Kalra and Dr. J.S. Goela for their invaluable guidance and encouragement throughout my thesis work.

I take this opportunity to express sincere thanks to all my friends for creating a congenial atmosphere and making my stay at IIT enjoyable and memorable.

Dinesh Kumar Jain

CONTENTS

Page

LIST OF SYMBOLS

A	Cross sectional area
A_{ij}	Rate of spontaneous emission from level j to i
c	Velocity of light in vacuum
C_p	Specific heat
C_R	Cooling rate per unit volume
D	Tube diameter
E_i	Energy of the ith level
E_t	Translational energy
E_{R1}	Energy removed in radiation zone
E_{R2}	Energy removed in post radiation zone
F	Radiation escape factor
F_{21}	Radiation escape factor corresponding to levels 1 and 2
F_{34}	Radiation escape factor corresponding to levels 3 and 4
F_n	Fibonacci number
$g(o)$	Line shape function
g_i	Degeneracy of level i
h	Convective heat transfer coefficient
I	Laser intensity
k	Boltzmann constant
K	Thermal conductivity
k_o	Absorption coefficient at the center of the line
k_o^{co}	Absorption coefficient at the center of the line for CO corresponding to levels 1 and 2
$k_o^{co_2}$	Absorption coefficient at the center of the line for CO_2 corresponding to levels 3 and 4

k_{ij} (i=2,3, j=1,4) Rate constant when the particle makes a transition from the state i to state j

k_{23}, k_{32} Rates for resonance energy transfer between levels 2 and 3

L Length of the tube

m Mass of one atom or molecule

M_i Molecular weight of species i

n_i Number density of ith level

n_T Total number density

n_{io} Number density of level i at the beginning of post radiation zone

p_i Pressure of ith species

p_T Total pressure

r Defined as $r = n_G/n_T$

R Universal gas constant, Tube radius

R_i Gas constant for species i

s Saturation parameter, $s = n_2/n_G$

T Absolute temperature

ΔT Temperature difference

τ Parameter defined as $\tau = x/u$

u Flow speed

W_{12}, W_{21} Stimulated absorption and emission rates respectively for levels 1 and 2

x Distance

λ_{ij} Wavelength corresponding to transition j i

$\Delta\Theta_1$	Temperature drop in the radiation zone
$\Delta\Theta_2$	Temperature drop in the post radiation zone
η	Refractive index
ν	Frequency
$(\Delta\nu)_D$	Doppler width

ABSTRACT

In this study, steady state cooling of a mixture of CO and CO_2 using laser radiation has been investigated for industrial applications. The basic cooling scheme involves exciting CO molecule with a frequency doubled CO_2 laser, resonance energy transfer to CO_2 upper laser level followed by fluoresence emission to the ground state of CO_2. The system configuration consists of a tube through which the mixture of CO and CO_2 flow while a circular laser beam falls perpendicular to the tube. Appropriate equations have been developed to calculate cooling rate in the radiated as well as post radiated zones. In the analysis, the effect of radiation trapping has also been included.

Our results show that cooling is produced in both radiated and post radiated zones when the total pressure is less than 200 mtorr. Further, the cooling rate is a function of pressure and tube radius; cooling rates are lower for smaller tube radii. The maximum volumetric cooling rates are in the range of 6-90 W/M and are obtained for pressure 90-100 mtorr and tube radii 1-2 cm.

LIST OF FIGURES

Table LIST OF TABLES Page

CHAPTER 1

INTRODUCTION AND LITERATURE SURVEY

1.1 INTRODUCTION

Low pressure gases could be cooled using a conventional heat exchanger wherein a coolant is passed over a container which encloses the gas to be cooled. In a conventional heat exchanger we rely on convective as well as conductive modes of heat transfer. For sufficiently large velocities, the conductive heat transfer is small as compared to the convective heat transfer. The various parameters which influence the convective heat transfer rate in a conventional system are the geometry, the Reynolds number and the Prandtl number. However, for a fully developed laminar flow in a channel, the heat transfer rate is independent of Reynolds and Prandtl numbers [1]. Essentially, the conventional systems are based upon surface cooling.

In the recent past, several schemes have been proposed for cooling low pressure gases using laser radiation [2-8]. A majority of them propose to reduce the thermal velocity of atoms or molecules, thereby reducing the Doppler width. These schemes, therefore, have applications in high resolution spectroscopy. A different scheme of laser induced cooling has also been proposed in ref. [8] and this scheme has applications in

Photon engine. In this work, a laser cooling scheme proposed recently [7] has been extended for bulk cooling for industrial applications.

The scheme analysed consists of pumping an excited state of an atom or molecule followed by near resonant energy transfer to another atom or molecule which then reradiates at higher or lower frequencies. Since the resonant energy exchange process can take place over the entire volume of the gas radiated by the laser beam, bulk cooling can take place. Bulk cooling has an advantage in achieving uniformity in heat exchange as compared to a conventional system where temperature differences within the volume are bound to occur.

Another advantage of the scheme analysed in the present work is that cooling can be achieved remotely without another fluid being brought in contact. This may find application in cooling in hazardous environment as in nuclear reactors. It could also be applied in outer space where a laser beam housed in a satellite can effect cooling on another satellite or a planet. At some places where local cooling is required, this system will prove to be very effective, whereas it will be difficult to achieve the desired results using conventional systems.

An important feature of this cooling system is that it is independent of the flow geometry and thermal properties such as thermal conductivity. Therefore, it could find applications in uniform cooling of a mixture of gases, in which the constituent gases have wide ranging thermal properties.

In this work, we have considered an actual system which will use laser radiation to cool a mixture of flowing gases. In this system, the laser beam is located perpendicular to the flow direction. The cooling effect in the radiated zone and the after effects have been calculated taking radiative trapping into account. Comparison with the conventional system has been made and discrepancies are discussed. Further, those regions over which laser cooling will be more effective than the cooling in conventional systems have been explored.

In Chapter 2 the basic principle used in effecting laser cooling is discussed and appropriate rate equations are derived. In addition an expression for cooling rate which takes into account radiative trapping has also been developed. In Chapter 3, the variables on which the cooling rate is dependent are identified. These variables are then optimized to get maximum cooling rate. In Chapter 4, the post-radiation zone has been explored and the heat removal in it is computed. Chapter 5 contains the laser power calculations. It also shows the comparison of this system with a conventional system. Summary,

conclusions and recommendations for future work are included in Chapter 6.

1.2 LITERATURE SURVEY

In the literature one finds essentially two types of cooling schemes using lasers : transient cooling and steady state cooling schemes, The transient cooling schemes are based upon one of the effects : radiative recoil [2,3], collisionally aided Flourescence [4] and the storage of energy in a vibrationaly stable mode [8]. Hansch and Schawlow [2] were the first to propose such a scheme in which it has been shown that magnesium vapours at a temperature of 600°, when illuminated by intense light on the low frequency side of the Doppler broadened singlet resonance line at $2852.1^{\circ}A$, would result in a reduction in the average velocity by a factor of 50 and a $.24^{\circ}K$ drop in the temperature. A system for generating an optical trap with a capacity of $3x10^{7}$ atoms and trapping rate $\backsim 10^{6}$ atoms/sec, using beams tuned 50 γ_N (natural line width) below the sodium D resonance frequency with a CW power 200 mW, has been proposed by Ashkins [3]. This could result in average velocity $\backsim$ 3 cm/sec which is equivalent to $10^{-6^{\circ}}K$.

The steady state cooling methods make use of multilevel systems and are based on : absorption of laser radiation followed by reradiation at higher frequencies [5,6] and resonant

energy transfer by an excited atom or molecule to another atom or molecule which then radiates at higher frequencies [7]. In all these schemes radiative trapping has been ignored. Djeu [5] has proposed to use laser radiation to resonantly excite P branch transition on higher J number in a molecular gas. The excited gas flouresces on P,Q and R branch transitions on low J number, releasing some of the photons of higher energy. The difference in energy is taken from the translational degree of freedom. For a Xe rich mixture using a 1 watt laser, he has evaluated the temperature difference between the wall of the tube and the axis as $\Delta \backsim .1$ r, if r is expressed in cm. Goela and Thareja [6] have proposed a scheme of using laser radiation to resonantly excite molecules having high Frank Condon factors but lower frequencies and getting reradiation on high Frank Condon factor but higher frequencies. The scheme is such that it could also be used for effecting cooling in high pressure gases. For a CN molecule, pumped with a tunable laser in the wavelength range 4159.6 A^{o} to 4208.2 A^{o}, they have evaluated the heat removal rate as $\backsim 10^{-13}$ cal S^{-1} per excited molecule for a laser power $\backsim 10^{3}$W and pulse energy $\backsim 10^{-3}$J. Goela and Thareja [7] have proposed another scheme of using resonant energy transfer to produce cooling in a mixture of gases. For a

mixture of CO and CO_2 at .1 torr, they have calculated a heat removal rate of .286 mW using a frequency doubled CO_2 laser of .5 mW. This scheme has also been used in this study for producing bulk cooling in a gaseous mixture of CO and CO_2 (as discussed in details in Chapter 2).

CHAPTER 2

ENERGY REMOVAL IN THE RADIATED ZONE

2.1 INTRODUCTION

In this chapter, we have outlined the procedure which we have followed in making energy removal calculations in a laser irradiated zone. First we have discussed how cooling effect is produced with a laser. Then a schematic representation of the proposed system is shown. A small note on rate constants is followed by the derivation of the governing equations which will be used in later chapters for detailed calculations.

2.2 LASER INDUCED COOLING

Laser is a source of intense energy. Therefore, one would expect to produce heating with it. However, under certain conditions, the resonance interaction between laser and atoms/molecules may also produce bulk cooling of the gas. This could be understood from Fig. 2.1. Here G and H are two species of atoms or molecules and 1,2,3 and 4 could either be electronic energy levels, vibrational levels or rotational levels. A laser of appropriate frequency excites atoms/molecules of G from level 1 to level 2. The excited atoms/molecules of G collide with those of H in energy level 4, and resonant energy transfer takes place as given below.

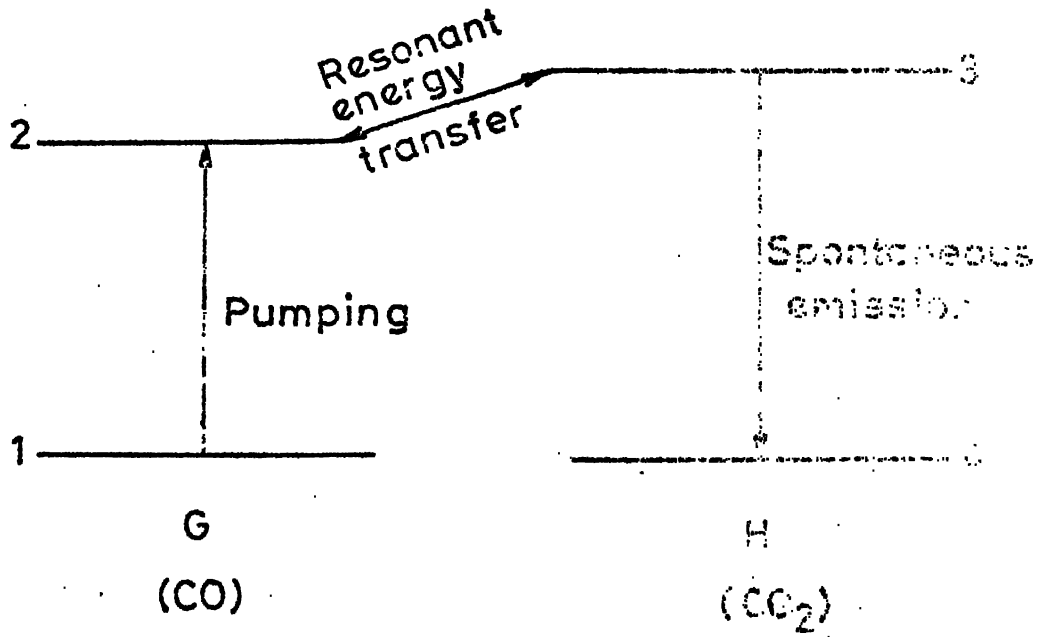

Fig. Scheme of producing steady state lasing through energy transfer

$$G(2) + H(4) \longrightarrow G(1) + H(3) - \Delta E \qquad (2.1)$$

where E is the energy difference given by

$$E = (E_3 - E_4) - (E_2 - E_1) = (E_3 - E_2) \qquad (2.2)$$

where E_i ($i = 1$ to 4) is the energy of the ith level. Both E_1 and E_4, being the energies in the ground states, may be taken to be zero relatively.

Once the atoms/molecules of H are excited to level 3, they decay to level 4 via spontaneous emission. For cooling it is necessary that $(E_3-E_4) > (E_2-E_1)$, so that ΔE is positive in eqns. (2.1) and (2.2). Cooling of the mixture is observed because a part or whole of this spontaneous radiation leaves the system. The cooling effect is brought about by a decrease in the translational energy of the gaseous mixture.

In this work the cooling scheme for industrial applications is centred around the above scheme. The species will G will represent the gas CO and H the gas CO_2. The level 2 of CO corresponds to 2143 cm^{-1}, and level 3 of CO_2 is at 2349 cm^{-1}. Accordingly

$$\Delta E_{12} = E_2 - E_1 = 4.26 \times 10^{-20} \text{ J} \qquad (2.2a)$$

and

$$\Delta E_{34} = E_3 - E_4 = 4.67 \times 10^{-20} \text{ J} \qquad (2.2b)$$

As a result,

$$\Delta E_{32} = E_3 - E_2 = 0.41 \times 10^{-20} \text{ J} \qquad (2.2c)$$

Since $E_{32} > 0$, cooling can be achieved, provided other conditions are favourable, as we will explore in detail later in this chapter as well as in Chapter 3.

2.3 SCHEMATIC REPRESENTATION OF LASER COOLING SYSTEM

A flow system, in which the gaseous mixture to be cooled is brought to interact with the laser radiation, will provide steady state cooling. The geometry as shown in Fig. 2.2 explains the scheme further. It essentially consists of a tube of radius R through which the gaseous mixture ($CO + CO_2$) flows at a flow speed u. The laser beam is also circular in cross section having a radius R and it falls perpendicular to the direction of flow. It is obvious that if the laser beam has the same radius as the tube, the interaction between the gaseous mixture and the laser would be maximum. A beam with radius greater than R, would remain partially unutilized.

Before we proceed to evaluate the rate of change of translational energy, it will be illuminating to first present a small note on vibrational relaxation rates and resonant energy transfer.

2.4 VIBRATIONAL RELAXATION

Considerable experimental information is available on the rates of exchange of energy between the vibrational and translational modes of diatomic molecules. In a mixture of

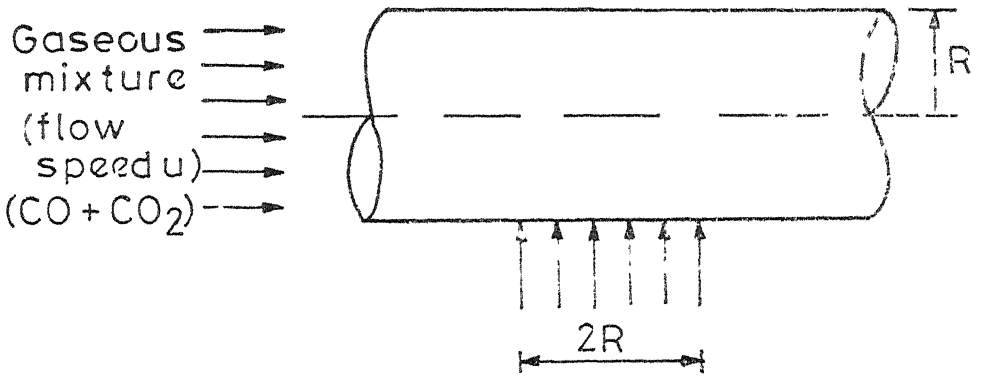

Fig 2·2 Schematic representation of laser cooling system

two gases (Fig. 2.1), the relaxation of the excited molecules of G and H can be represented by the following equations :

$$G(2) + X \rightarrow G(1) + X + \Delta E_{12} \qquad (2.3)$$

$$H(3) + X \rightarrow H(4) + X + \Delta E_{34} \qquad (2.4)$$

where X is any molecule of the mixture, and ΔE_{12} and ΔE_{34} are as given in eqn. (2.2a) and (2.2b).

This, in reality, is a simplified way of visualizing the relaxation process which allows it to be characterized by two rate constants only, viz., k_{21} (s^{-1}) for reaction (2.3) and k_{34} (s^{-1}) for reaction (2.4). This is in tune with the experimental information available on the rate constants, especially of the mixture of CO and CO_2, as will be dealt with in the present work.

Since X in eqns. (2.3) and (2.4) is any molecule of the mixture, the rate constants k_{21} and k_{34} will be considered as functions of the total pressure of the mixture. The actual reaction rates of reactions (2.3) and (2.4) will also depend on the partial pressures or number densities of G(2) and H(3), respectively. These will appear explicitly in Section 2.6, when the rate equations are written. At 300°K, the values of k_{21} and k_{34} are given by [9,10]

$$k_{21} = 10^{-2}\ p_T\ (s^{-1}) \qquad (2.5)$$

and

$$k_{34} = 193\ p_T(s^{-1}) \qquad (2.6)$$

where p_T is the total pressure of the mixture in torrs.

The rate constants k_{21} and k_{34} can easily be expressed as functions of the total number density n_T using the ideal gas relationship

$$p = nkT \qquad (2.7)$$

where

p = pressure in P_a

n = number density, m^{-3}

k = Boltzmann constant, 1.38×10^{-23} J/K

T = temperature, K,

and the conversion factor between torr and P_a (1 torr $\backsim$ 133 P_a). The resulting values are :

$$k_{21} = 3.105 \times 10^{-25}\ n_T \qquad (2.8)$$

and

$$k_{34} = 5.99 \times 10^{-21}\ n_T \qquad (2.9)$$

where k_{21} and k_{34} have units of s^{-1} and n_T in m^{-3}.

It may be pointed out here that these values should be considered applicable in the vicinity of 300K. Variation with temp. will not be accounted for in this work.

2.5 RESONANT ENERGY TRANSFER

The resonant energy transfer between energy level 2 of G and energy level 3 of H can be represented as follows :

$$G(2) + H(4) \longrightarrow G(1) + H(3) - \Delta E \qquad (2.10)$$

$$G(1) + H(3) \longrightarrow G(2) + H(4) - \Delta E \qquad (2.11)$$

where ΔE is as in eqn. (2.2).

The rate constant associated with (2.10) will be denoted by k_{23} (s^{-1}) and that associated with (2.11) by k_{32} (s^{-1}). These rate constants will be considered as functions of partial pressures of H(4) and G(1), respectively. The dependence of the actual reaction rates of (2.10) and (2.11) on G(2) and H(3), respectively, will be written explicitly in the rate equations in Section 2.6. This is in tune with the experimental data available, where, in fact these rate constants are given as function of total pressures. However, if significant change in level population is involved, these must be considered as depending on the respective ground level populations.

With this interpretation, the values of k_{23} and k_{32} are [9] :

$$k_{23} = 1.38 \times 10^{3}\ p_1\ (s^{-1}) \qquad (2.12)$$

and

$$k_{32} = 3.68 \times 10^{3}\ p_4\ (s^{-1}) \qquad (2.13)$$

where p_1 and p_4 are the partial pressures in torr of molecules in energy levels 1 and 4, respectively.

As in Section 2.4, k_{23} and k_{32} can be expressed as functions of number densities n_1 and n_4 of the respective levels :

$$k_{23} = 4.285 \times 10^{-20} \, n_1 \qquad (2.14)$$

and

$$k_{32} = 11.42 \times 10^{-20} \, n_4 \qquad (2.15)$$

where k_{23} and k_{32} are in units of s^{-1} and n_1 and n_4 are in m^{-3}.

2.6 RATE EQUATIONS

As pointed out earlier, the cooling effect is a result of decrease in the translational energy of the gaseous mixture. The rate of change of translational energy of the gas per unit volume can be written as

$$\frac{dE_t}{dt} = n_2 k_{21} (E_2 - E_1) + n_3 k_{34} (E_3 - E_4)$$

$$- n_2 k_{23} (E_3 - E_2) + n_3 k_{32} (E_3 - E_2) \, , \qquad (2.16)$$

where

E_t = translational energy of the gas mixture, J/m^3,

n_i = number density of molecules in level i, i = 1 to 4, m^{-3},

and k_{ij} are the rate constants as explained earlier.

The population n_1 of various energy levels depends upon the laser pumping and other energy transfer mechanisms. These populations, for the radiated zone, may be calculated from the following equations :

$$\frac{dn_2}{dt} = W_{12}n_1 - W_{21}n_2 - n_2k_{21} - n_2k_{23} + n_3k_{32} - n_2A_{21} \qquad (2.17)$$

$$\frac{dn_3}{dt} = -A_{34}n_3 + K_{23}n_2 - K_{32}n_3 - n_3K_{34} \qquad (2.18)$$

$$n_1+n_2 = n_G \qquad (2.19)$$

$$n_3+n_4 = n_H \qquad (2.20)$$

where

W_{12}, W_{21} are the rates of stimulated absorption and emission respectively, between levels 1 and 2, s^{-1}

A_{21} is the rate of spontaneous emission from level 2 to 1, which for CO for the levels in Fig. 2.1, is 33.8 s^{-1} [10]

A_{34} is the rate of spontaneous emission from level 3 to level 4, which for CO_2, for the levels in Fig. 2.1, is 400 s^{-1} [10].

n_G is the number density of gas G in m^{-3} which is CO in the present work

n_H is the number density of gas H in m^{-3}, which is CO_2 in the present work

Also,

$$n_H + n_G = n_T \tag{2.21}$$

where

n_T is the total number density (m^{-3}) as explained in Section 2.4.

The eqns. (2.17) and (2.18), however, should be modified to take into account radiation trapping. This is explained in the next section where appropriate modifications are introduced.

2.7 RADIATION TRAPPING

In radiation trapping, a photon emitted by an excited atom/molecule is absorbed by another atom/molecule, reemitted, reabsorbed and so on. This reduces the effective rate of spontaneous emission of radiation from A_{ij} to FA_{ij} [11]. According to Holstein's analysis for cylindrical geometry and Doppler broadening,

$$F = \frac{1.60}{k_o R(\pi \log k_o R)^{1/2}} \tag{2.22}$$

where R is the tube radius (m),

k_o is the absorption coefficient, m^{-1}, at the center of the line given by the expression :

$$k_o = g(o)\left(n_i - \frac{g_i}{g_j} n_j\right) \tag{2.23}$$

where

$$K = \frac{\lambda_{ij}^2 \, A_{ji}}{8\pi\eta^2} \, \frac{g_j}{g_i} \quad , \tag{2.23a}$$

λ_{ij} is the wavelength corresponding to the transition j → i,

A_{ji} is the spontaneous transition probability,

η is the refractive index of the medium,

g_i is the degeneracy of level i, and

g(o) is the line shape function.

For the case of Doppler broadening, the line shape function, g(o) is given by

$$g(o) = \frac{2}{\Delta\nu_D} \left(\frac{\log 2}{\pi}\right)^{1/2} \tag{2.24}$$

$\Delta\nu_D$ is the width of the Doppler broadened line (full width at half maximum) given as

$$(\Delta\nu)_D = \frac{2\nu_o}{c} \left(\frac{2kT \log 2}{m}\right)^{1/2} \tag{2.25}$$

where

m is the mass of the atom or molecule, ν_o is the frequency corresponding to the transition j → i,

k is the Boltzman's constant,

T is the temperature of the gas in Kelvin and

c is the velocity of light in vacuum.

In an actual situation factors producing both types of broadening i.e., Doppler as well as collision broadening may be

present at the same time. However, at low pressures, it is the Doppler broadening that dominates. As will be seen shortly, pressures of interest to us are sufficiently low. Hence, only Doppler broadening effect has been taken into account in the calculation of the radiation escape factor F.

The range for the values of F is from 0 to 1. The extreme case of F being equal to zero is when no radiation leaves the system. Physically, this will be the case when the number densities are large and/or the tube radius is large. The other extreme of F being equal to one occurs when the number densities are very low and/or the tube radius is small and all the radiation manages to escape from the system.

Hence, from now on, we will work with $F_{ij}\ A_{ij}$ instead of A_{ij}, F_{ij} accounting for the trapping of radiation corresponding to transition between the states j and i.

2.8 GOVERNING EQUATIONS

The modified rate equations can be written as

$$\frac{dn_2}{dt} = W_{12}n_1 - W_{21}n_2 - n_2k_{21} - n_2k_{23} + n_3k_{32} - F_{21}A_{21}n_2 \qquad (2.26)$$

$$\frac{dn_3}{dt} = -F_{34}A_{34}n_3 + k_{23}n_2 - k_{32}n_3 - n_3k_{34} \qquad (2.27)$$

For the steady state condition, there is no change in the population of level 2 and 3, i.e.,

$$\frac{dn_2}{dt} = 0, \qquad \text{and} \qquad \frac{dn_3}{dt} = 0 \tag{2.28}$$

Therefore, on solving the above equations, we obtain

$$n_3 = \frac{k_{23}\, n_2}{k_{34} + k_{32} + F_{34}\, A_{34}} \tag{2.29}$$

$$n_2 = \frac{W_{12} n_G}{\left[(W_{12}+W_{21}+F_{21}A_{21}+k_{21}+k_{23}) - \dfrac{k_{23}k_{32}}{F_{34}A_{34}+k_{32}+k_{34}}\right]} \tag{2.30}$$

where use of eqn. (2.19) has also been made.

To explore the conditions under which cooling can take place, we make use of eqn. (2.29) in eqn. (2.16) to write the latter as :

$$\frac{dE_t}{dt} = n_3(E_2-E_1).\left[(F_{34}A_{34}+k_{32}+k_{34})\,\frac{k_{21}}{k_{23}} + k_{34} - F_{34}A_{34}\,\frac{E_3-E_2}{E_2-E_1}\right] \tag{2.31}$$

For a mixture of CO and CO_2, as in our case, the first term in eqn. (2.31) involving k_{21} is likely to be negligible in comparison with the other two terms. This follows from an order of magnitude comparison of the values given in eqn. (2.8), (2.9), (2.14) and (2.15). This will be further confirmed in Chapter 3, where it will be shown that this term is indeed negligible for

the $CO-CO_2$ system under all operating conditions of interest.

We will, therefore, make simplifications by neglecting this term in all our calculations. Under these conditions,

$$\frac{dE_t}{dt} = n_3(E_2-E_1) \cdot \left[k_{34}-F_{34}A_{34}\frac{E_3-E_2}{E_2-E_1}\right] \tag{2.32}$$

Since $\frac{dE_t}{dt}$ is the rate of change of translational energy, cooling will be observed if $\frac{dE_t}{dt} < 0$, i.e.,

$$F_{34}A_{34}\left(\frac{E_3-E_2}{E_2-E_1}\right) > k_{34} \tag{2.33}$$

The upper limit of the pressure at which this condition will be satisfied can be obtained by assuming the radiation escape factor $F_{34} = 1$ and using the values given earlier, together with eqns. (2.6) or (2.9). The limiting total pressure is found to be 0.199 torr. In terms of the total number density of the mixture, it corresponds to $n_T = 6.42\times10^{21}$ m^{-3}.

Obviously, the actual operating pressures have to be below this limiting value. These, together with corresponding partial pressures, will be explored in detail in Chapter 3.

CHAPTER 3

OPTIMUM COOLING CONDITIONS

3.1 INTRODUCTION

In this section we will identify the factors on which the cooling rate depends. The variation in cooling rate as a function of these variables will be discussed. This will be followed by a brief note on the technique used to optimise cooling rate. Results using this technique are then presented in tabular as well as graphical form and subsequently, the total cooling effect and the resulting temperature drops are evaluated and discussed.

3.2 RADIATION ESCAPE FACTOR CALCULATIONS

The expressions for radiation escape factor F have been listed in Section 2.7. The relevant data and the numbers arrived at by using these expressions are presented below. For CO at 300°K corresponding to levels 1 and 2, we have,

$$
\begin{aligned}
A_{21} &= 33.8 \text{ sec}^{-1} \\
(\Delta\nu)_D &= 1.507\times10^{8} \text{ Hz} \\
\lambda_{12} &= \frac{1}{2143} \text{ cm} = 4.66\times10^{-6} \text{ m} \\
k_o^{CO} &= 1.824\times10^{-19} [n_1 - n_2] \text{ m}^{-1}
\end{aligned}
\qquad (3.1)
$$

and for CO_2 at 300°K, corresponding to levels 3 and 4,

$$A_{34} = 400 \text{ sec}^{-1}$$

$$(\Delta\nu)_D = 1.3177\times10^{8} \text{ Hz}$$

$$\lambda_{34} = \frac{1}{2349} \text{ cm} = 4.26\times10^{-6} \text{ m}$$

$$k_o^{CO_2} = 1.353\times10^{-18} (n_4 - n_3) \text{ m}^{-1} \qquad (3.2)$$

The values derived here are used to evaluate the radiation escape factors namely F_{21} and F_{34}. It may be indicated here that F_{21} is not needed for the radiation zone calculations, it is required later in Chapter 4 for the calculations in the post-radiation zone.

3.3 IDENTIFICATION OF VARIABLES

For the system presented in Fig. 2.2, it is easily seen that the cooling rate will depend on the following variables

a) Total pressure p_T (or number density n_T),

b) partial pressure of one of the constituent gases, p_{CO} or p_{CO_2},

c) flow speed u,

d) tube radius R, and

e) laser intensity I.

However, if we make the assumption that the characteristic residence time of a molecule in the radiation zone is sufficiently larger than the average relaxation time, the energy removal rate does not depend on the flow speed, u. As will be seen later, a result of this is that the temp. drop in the radiation zone is inversely proportional to u.

The dependence of the cooling rate on the tube radius R is only through the dependence of the radiation escape factor F_{34} on R, as can be seen from eqn. (2.22), In order to account for the dependence of the cooling rate on laser intensity, we introduce a parameter s which is a measure of saturation, as follows :

$$s = \frac{n_2}{n_G} \tag{3.3}$$

The maximum value of s is 0.5, which will occur if the laser beam is sufficiently intense. Otherwise $s < 0.5$.

Similarly, to account for the partial pressures of the two gases in the mixture, we introduce a parameter r defined as follows :

$$r = \frac{n_G}{n_T} \tag{3.4}$$

obviously, $o \leq r \leq 1$.

In terms of these parameters, we can write from eqn. (2.32) the following expression for the volumetric cooling rate, C_R (w/m^3) :

$$C_R = -\frac{dE_t}{dt}$$

$$= \frac{C_{23} \cdot s \cdot r \cdot (1-r) n_T^2 [F_{34} A_{34} \Delta E_{32} - C_{34} n_T \Delta E_{21}]}{[F_{34} A_{34} + (1-s) C_{32} r n_T + s C_{23} r n_T + C_{34} n_T]} \qquad (3.5)$$

where C_{34}, C_{23} and C_{32} are the numerical factors appearing in eqns. (2.9), (2.14) and (2.15), respectively. It is seen that C_R depends on s, r and n_T explicitly as well as implicitly through F_{34}, while dependence on R is only implicitly through F_{34}. We will first discuss the dependence of C_R on the parameter s, which is a measure of saturation between levels 1 and 2 as indicated above.

3.4 EFFECT OF THE SATURATION PARAMETER ON THE COOLING RATE

If F_{34} were not to depend on the saturation parameter s, it is easily seen from eqn. (3.5) that the cooling rate C_R will be a monotonically increasing function of s. Thus the maximum value of C_R will occur for the maximum value of s (i.e. s = 0.5), for any value of other parameters like, r, n_T and R. But in reality, s affects n_3 and n_4, which in turn affects F_{34}. Since the algebraic dependence is too complicated, quite cumbersome expressions are obtained if one pursues the matter analytically. We will therefore be satisfied by investigating

the dependence of C_R on s, numerically.

For this purpose, we calculate C_R for some given values of R, n_T and r, while continuously varying s from 0 to 0.5. The calculation procedure is shown in the form of a flow chart in Fig. 3.1. Most of the calculation involved is for evaluating F_{34} iteratively. The cooling rate is finally obtained using eqn. (3.5.).

The values of the cooling rate (w/m^3) are plotted in Fig. 3.2, for R = 0.5 cm, $n_T = 3 \times 10^{21}$ m^{-3} (p_T = 93 mtorr), and for two different values of r. It is seen that the maximum cooling rates are indeed achieved for s = 0.5, i.e., at the saturation condition. We will make a further comment on it in Section 3.7. Most of the remaining calculations in this work will be done for the saturation condition, for which C_R can be obtained by substituting s = 0.5 in eqn. (3.5) :

$$C_R = \frac{C_{23} r(1-r) n_T^2 [F_{34} A_{34} \Delta E_{32} - C_{34} n_T \Delta E_{21}]}{[2F_{34}A_{34} + (C_{23}+C_{32}) r n_T + 2C_{34} n_T]} \qquad (3.6)$$

3.5 OPTIMAL PRESSURE RATIO FOR A SPECIFIED TUBE RADIUS AND TOTAL PRESSURE

Figure 3.3 plots the cooling rate as a function of the parameter r, which is the ratio of the partial pressure of gas G (i.e., CO) to the total pressure of the mixture. This is done for a fixed tube radius, and two fixed values of the total

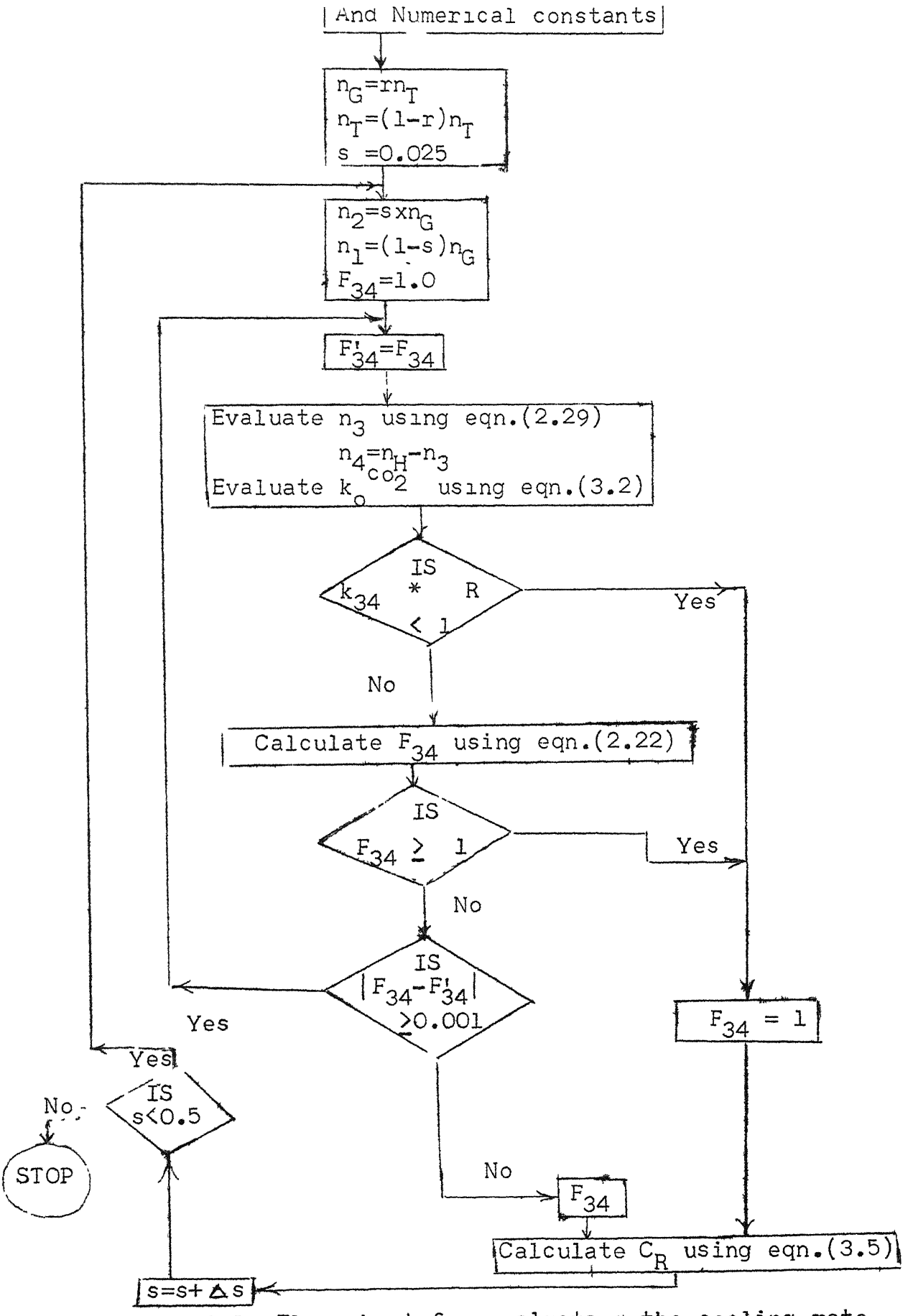

Fig.3.1 Flow chart for evaluating the cooling rate for given values of parameters, R, n_T and r with a consistent calculation for F_{34}

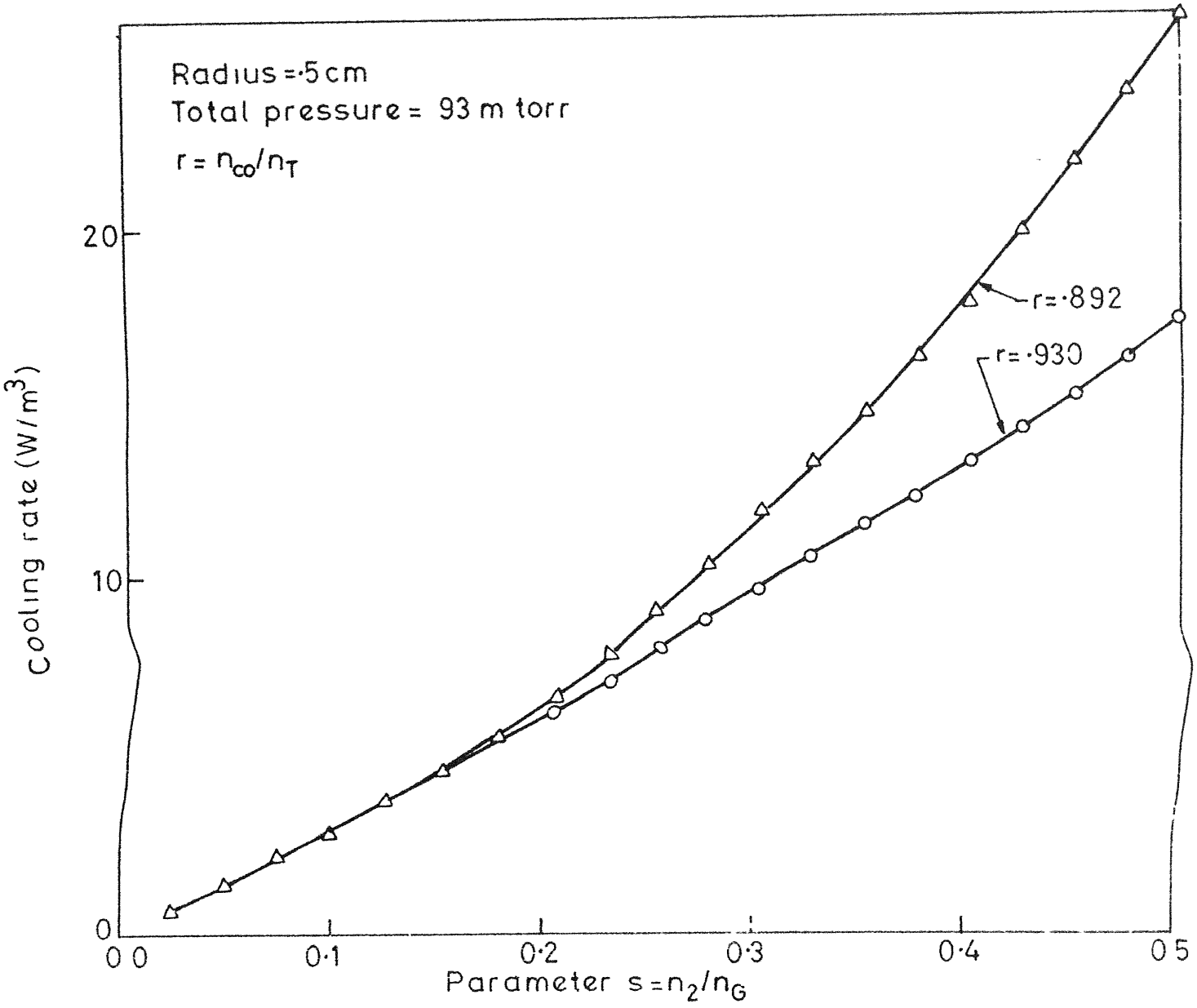

Fig 3 2 Volumetric cooling rate at different conditions of saturation

pressure. The calculations are, of course, done for the saturation condition, i.e. s = 0.5.

It is seen that for given values of tube radius and total pressure, there is an optimal value of r which leads to maximum cooling rates. This is also brought out from eqn. (3.5) or eqn. (3.6), which shows that $C_R = 0$ for r = o, and also for r = 1, indicating one or more extremal points between r = o and 1.

It should also be noted that for a given value of n_T (or p_T), there may be cooling for all values of r, or there may be heating for some values of r, and cooling for other values of r, as is clear from Fig. 3.3. In Fig. 3.4 we also show the corresponding radiation escape factors. It is seen that F_{34} increases as r increases, which is to be expected, because increase in r signifies decrease in CO_2 gas.

We have plotted Figs. 3.3 and 3.4 in detail for illustration only. Otherwise, our interest lies in identifying, for given values of R and n_T, that value of r which will provide maximum cooling rate. Towards this end, we use an optimization scheme based on Fibonacci method [12]. This is discussed in Section 3.6, and the results obtained are discussed in Section 3.7.

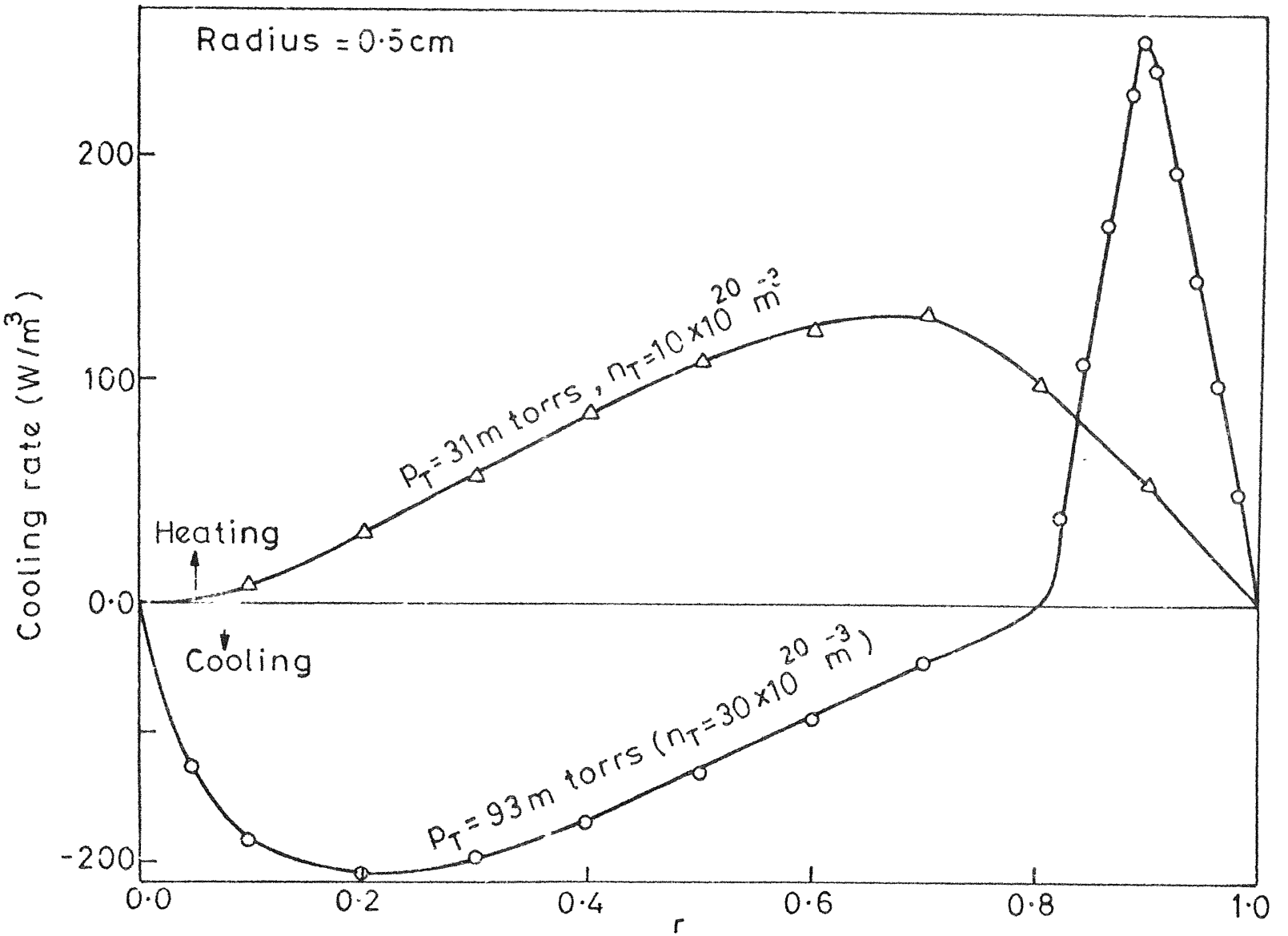

Fig.3-3 Variation of cooling rate with $r = n_G / n_T$

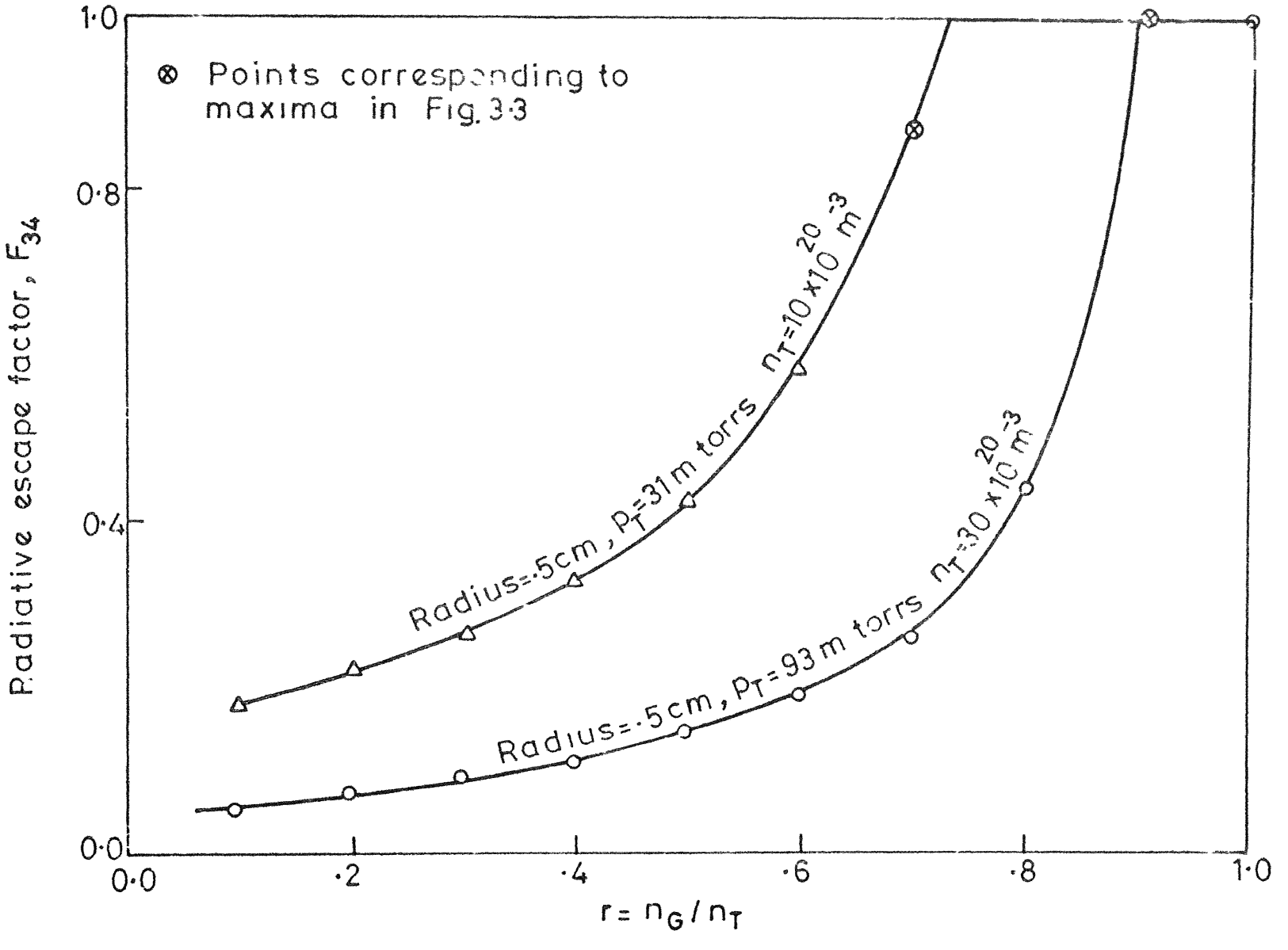

Fig. 3·4 Radiation escape factor F_{34} as a function of r

3.6 FIBONACCI METHOD

This method can be used to find the minimum or maximum of a function of one variable, even if the function is not continuous. This method has the following limitations.

(i) The initial interval in which the optimum lies, has to be known. In our case this is known because $o \leq r \leq 1$.

(ii) The exact optimum can not be located. Only an interval, known as the final interval of uncertainity will be known. The final interval of uncertainity can be made as small as desired by making more computations.

This method makes use of the sequence of Fibonacci numbers, F_n, defined as

$$F_o = F_1 = 1$$

and $$F_I = F_{I-1} + F_{I-2}, \quad I = 2,3, \ldots, N \qquad (3.7)$$

yielding a sequence 1,1,2,3,5,8,13 ....

It essentially consists of comparing the values of the function at two points, that are specified using Fibonacci numbers, in the interval of uncertainity. A portion of this interval is discarded based on this comparison and the value of the function at a new point (again specified using Fibonacci numbers) in the remaining interval is evaluated. A comparison is made again and the process is continued till a desired interval of

uncertainty is achieved. The optimal can lie anywhere within this final interval. By choosing N = 20, we can calculate the value of r with an accuracy of better than $\pm$ 0.0001.

The flow chart is given in Fig. 3.4. Here A_1 and B_1 are the extreme limits of the variable r, i.e., $A_1 = 0$ and $B_1 = 1$, and N = 20. The program based on this chart will calculate that value of r, i.e., (n_G/n_T), for which cooling rate is maximum, for a given value of tube radius (R) and total number density (n_T). As can be seen from the chart, R and n_T are used as input values.

The cooling rate C_R is given by eqn. (3.6) if s = 0.5, or eqn. (3.5) if s < 0.5. The scheme used to obtain a consistent value of F_{34} for evaluating the cooling rates is same as in Fig. 3.1. It may also be pointed out that various other values of interest, e.g., n_3,n_4 etc. can also be obtained using the flow chart shown in Fig. 3.2. As will be seen later, these values are required as input conditions to the post radiation zone.

This exercise has been repeated for various values of R and n_T. The results thus obtained are presented and discussed in the next section.

3.7 RESULTS AND DISCUSSION

Using the Fibonacci method we can obtain the maximum cooling rates corresponding to the various values of n_T for

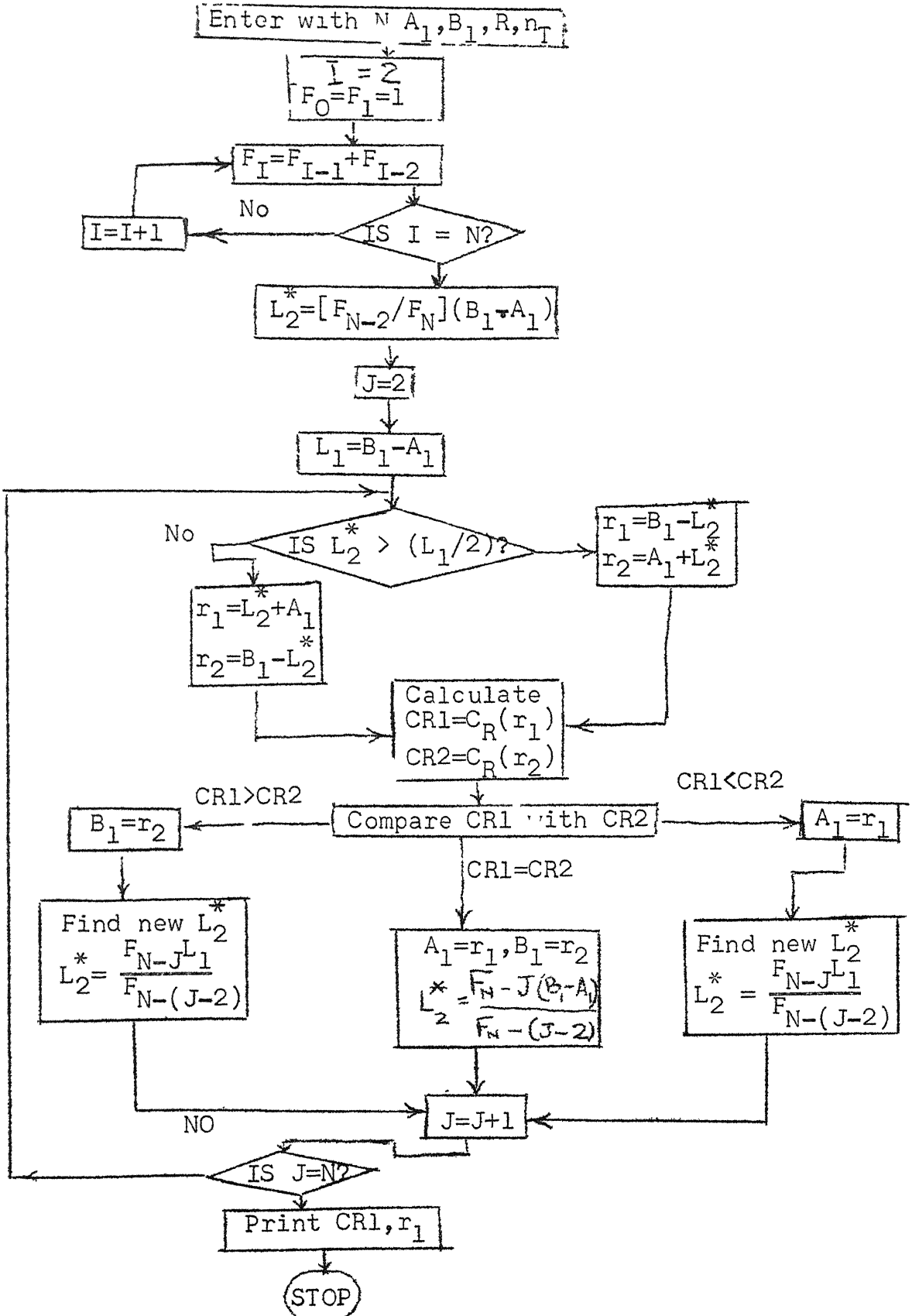

Fig. 3.5 Flow chart for calculating optimal value of r by Fibonacci method

Table 3.1

A set of values obtained using Fibonacci method

Tube radius .5 cm

$n_T \times 10^{-20}$ (No./m^3)	p_T (mtorrs)	r (n_G/n_T)	Cooling rate (W/m^3)
5	15.5	0.4884	4.78
10	31.0	0.6856	13.10
15	46.6	0.8026	18.90
20	62.0	0.8472	22.90
25	77.0	0.8738	25.10
30	93.0	0.8919	25.80
35	108.0	0.9051	25.06
40	124.0	0.9150	23.10
45	139.0	0.9229	20.00
50	155.0	0.9293	16.00
55	170.0	0.9347	11.00
60	186.0	0.9392	5.30
65	202.0	0.9990	-0.0018

different tube radii, and the corresponding values of the parameter r. Table 3.1 shows the results of this exercise for a tube radius 0.5 cm. Similar values have been obtained for other tube radii.

From Table 3.1, we can easily see that maximum achievable cooling rate for this tube radius is achieved for $n_T = 30x10^{20}/m^3$ (or p_T = 93 mtorrs) and at r = 0.892. Since at these values maximum cooling is achieved, we call these conditions as optimum operating conditions. The cooling rate attained with these values is 25.8 w/m^3. The total pressure p_T is calculated using ideal gas relationship p = nkT, for T = 300 K, where k is the Boltzmann constant. In Fig. 3.6, the values of the maximum cooling rates are shown for the saturated and unsaturated conditions. Once again, it is seen that the maximum cooling rates are achieved for the saturation condition.

Figure 3.7 shows maximum cooling rate as a function of total pressure for tube radii 0.1 cm and 1 cm. Fig. 3.8 shows the same for tube radii 1 cm and 2 cm. From these two plots, it is easily seen that maximum achieveable cooling rate per unit volume is the highest for tube radius 0.1 cm. This is so because for low radius of the tube, the radiation trapping is low and a significant amount of radiation leaves the system.

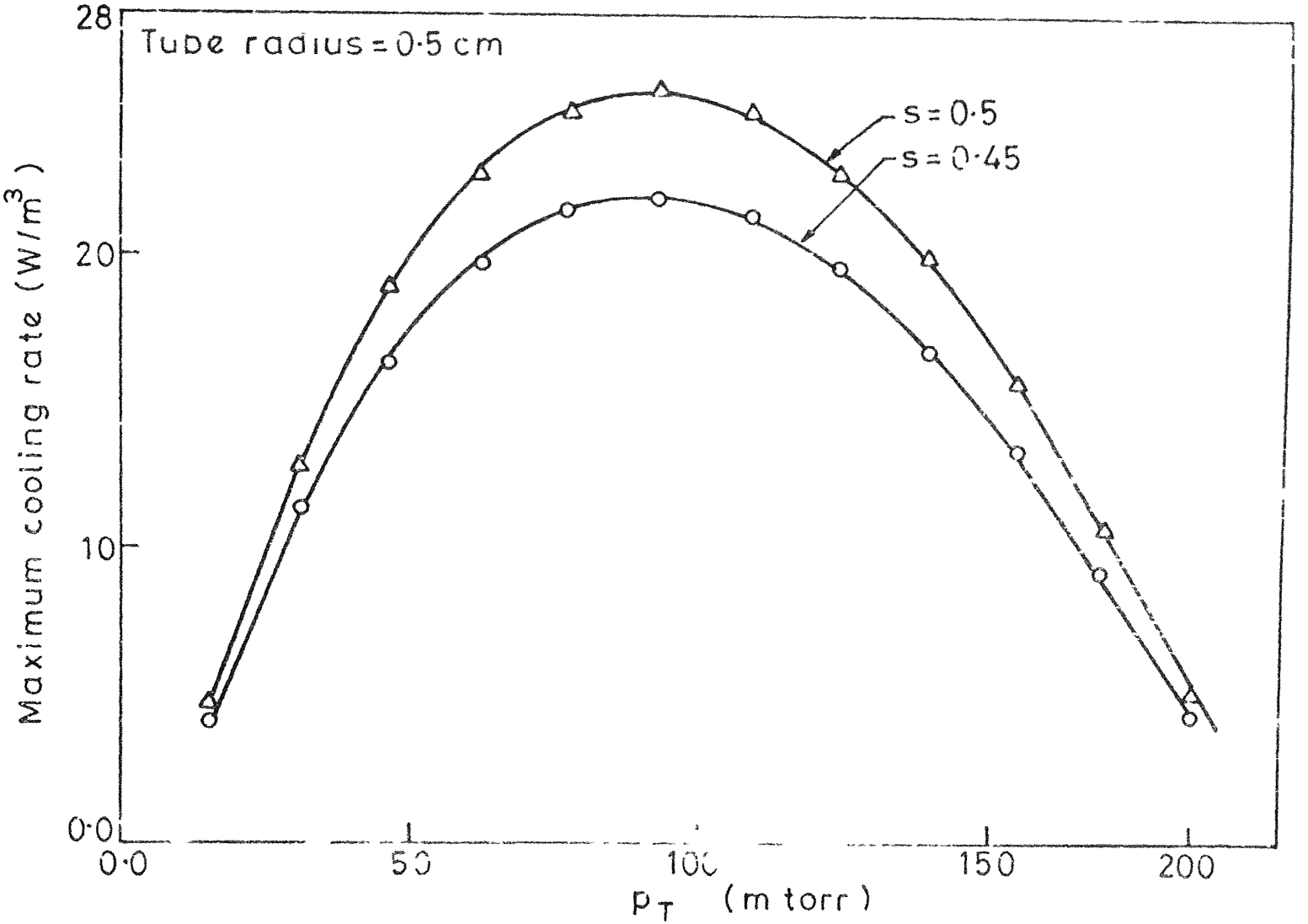

Fig 3 6 Maximum cooling rate as a function of total pressure for saturated and unsaturated conditions

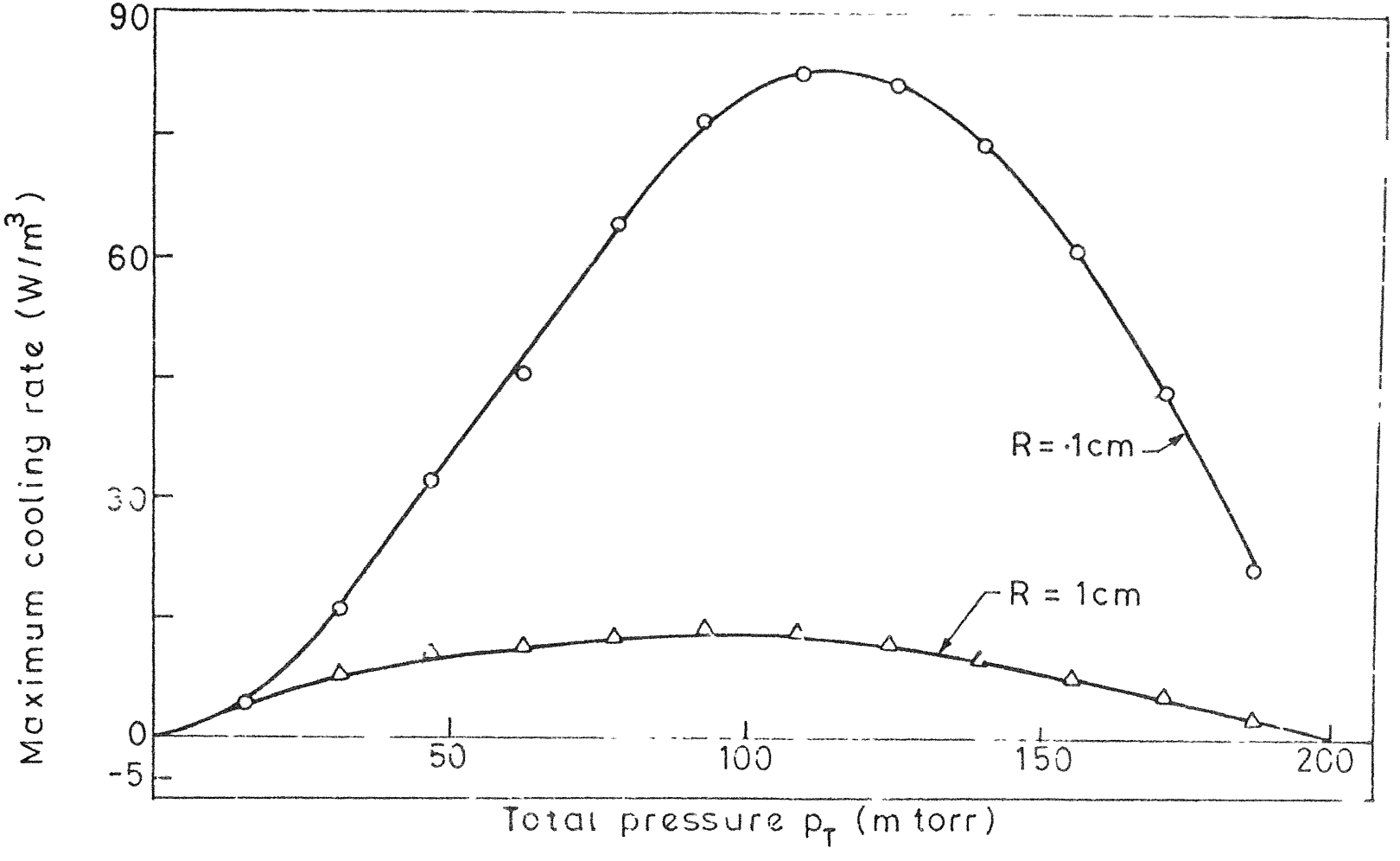

Fig. 3·7 Comparison of maximum cooling rates for R=0·1 and 1cm

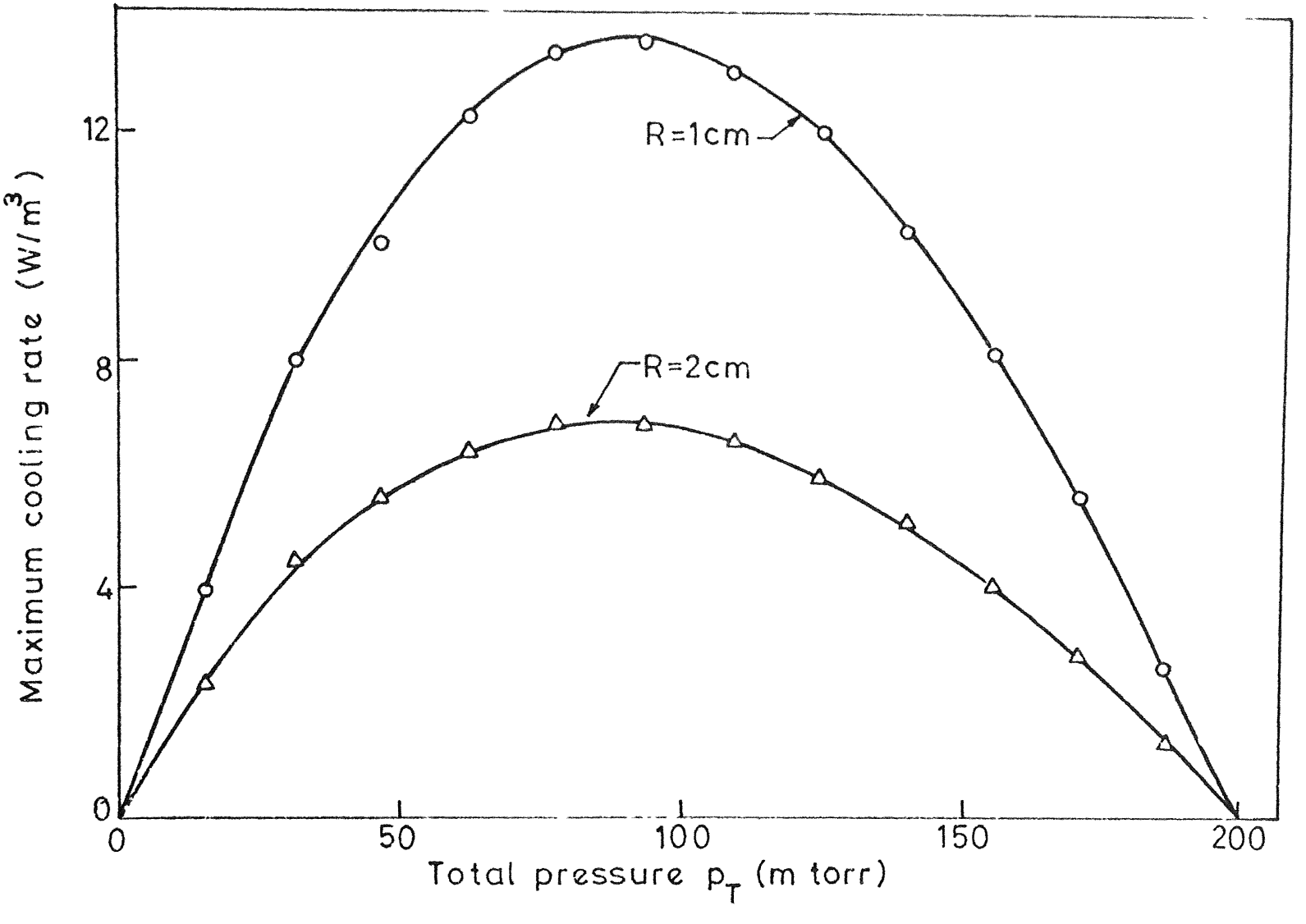

Fig.3·8 Comparison of maximum cooling rates for R=1 and 2cm

Figure 3.9 shows the optimal conditions p_T and r with tube radius as a parameter. The optimal r increases with increasing tube radius. This is so because as the tube radius increases, the radiative trapping increases. One way to decrease this effect is by reducing the amount of CO_2 gas present in the system. Increase in r has the effect of lowering the CO_2 content of the mixture. This however is not necessarily required for low tube radii operating at low pressures, as is seen from the plot for R = 0.1 cm at lower values of p_T in Fig. 3.9.

From representative detailed data presented above, the following points are clearly brought out :

(a) Corresponding to each tube radius, there is an optimum total pressure of the mixture, which leads to maximum cooling rate per unit volume.

(b) In order to achieve this maximum cooling rate, the partial pressures of the two gases should have a definite value.

These results are given in Table 3.2. Also listed in this table are the total cooling rates, E_{R1}, obtained as follows :

$$E_{R1} = \frac{1}{\sqrt{\pi}} \; D^3 \; C_R \qquad (3.8)$$

where C_R is the volumetric cooling rate, W/m^3. These results are also shown in Figs. 3.10 and 3.11.

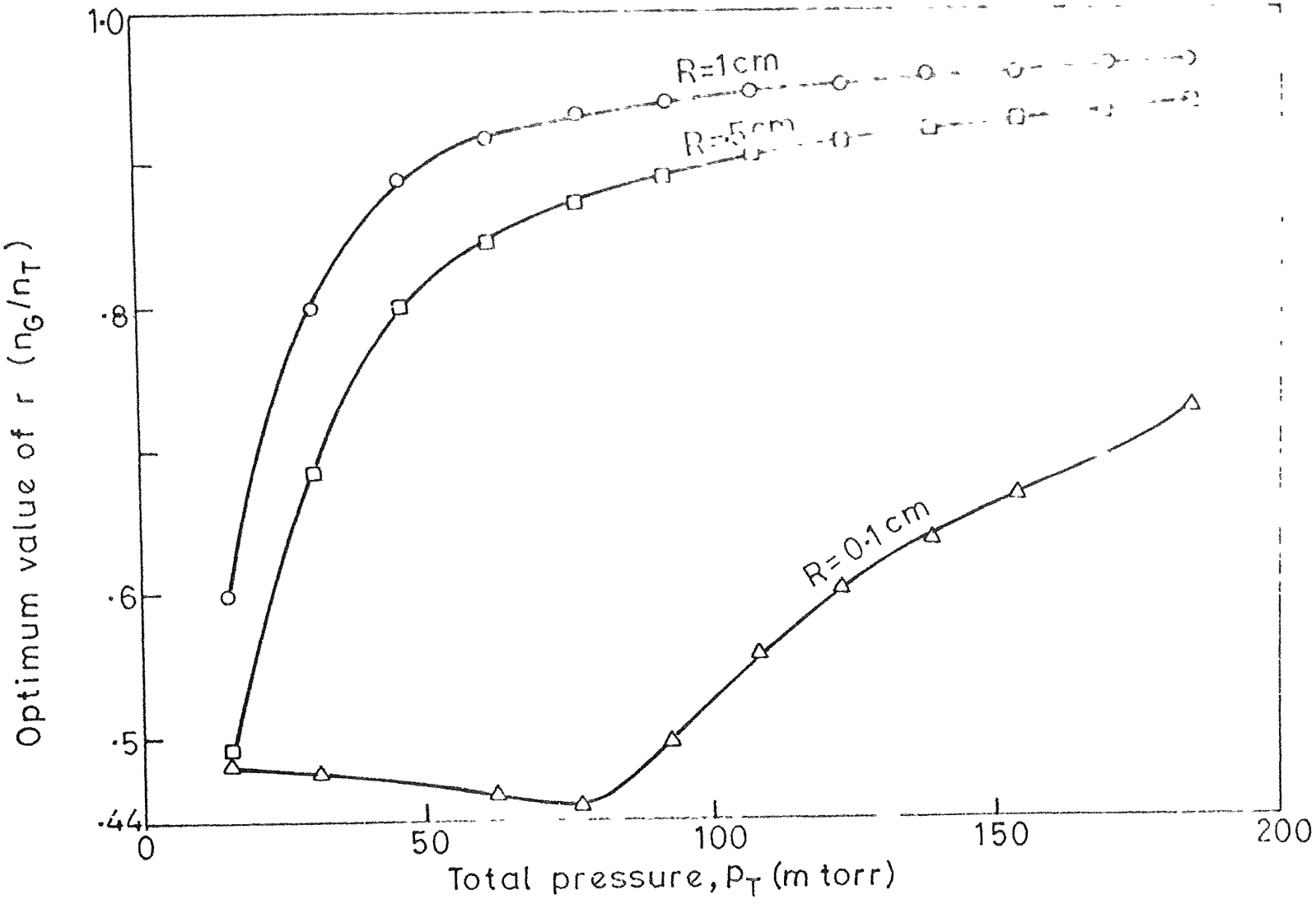

Fig.3·9 Optimum value of r for different tube radius and operating pressures

Table 3.2

Optimal total pressure, partial pressure and maximum achievable cooling rates for different tube radii

S.No.	Radius, R (cm)	Optimum total pressure, p_T	Optimum $r=(p_{co}/p_T)$	Cooling rate, C_R (w/m^3)	Total cooling rate, E_{RL} (w)
1.	0.1	97.9	0.557	84.0	0.30
2.	0.3	96.2	0.822	40.0	4.00
3.	0.5	92.7	0.892	25.0	14.50
4.	0.7	91.2	0.922	18.9	29.00
5.	0.9	90.0	0.940	14.9	49.00
6.	1.0	89.9	0.945	13.5	61.00
7.	1.1	89.6	0.950	12.3	74.00
8.	1.3	89.4	0.958	10.5	104.00
9.	1.5	89.1	0.963	9.1	139.00
10.	1.7	88.7	0.968	8.1	180.00
11.	1.9	88.5	0.971	7.2	225.00
12.	2.0	88.3	0.973	6.9	249.00
13.	2.1	88.3	0.974	6.6	275.00

3.8 EFFECT OF k_{21} ON THE COOLING RATES

As was pointed out in Chapter 2, Section 2.8, the term involving k_{21} in the cooling rate expression has been neglected in all our calculations (see eqns. (2.31) and (2.32)). It is easy to see the effect of this term on the cooling rate and the optimal operating conditions listed in Table 3.2. For example, for R = 1 cm, it can be seen that this term reduces cooling rates by approximately 0.05 W/ m^3. This is negligible compared to the actual cooling rate obtained, viz., 13.5 W/m^3.

Effect of this term is of the same order of magnitude for other operating conditions. Hence, neglecting it is entirely justified.

3.9 TEMPERATURE DROP IN THE RADIATION ZONE

Using the optimum cooling rates in the radiated zone, we will evaluate the temperature drop in this zone for various tube radii using the following expression :

$$[(\rho C_p)_{CO} + (\rho C_p)_{CO2}] \cdot A.u. \Delta\theta_1 = E_{R1} \qquad (3.9)$$

where, A is the area of cross section of the tube (m^2),

u is the flow speed (m/s),

$\Delta\theta_1$ is the temperature drop in the radiation zone,

and C_p are the density (kg/m^3) and the specific heat (J/kgK). The subscript denotes the species of which the properties must be used.

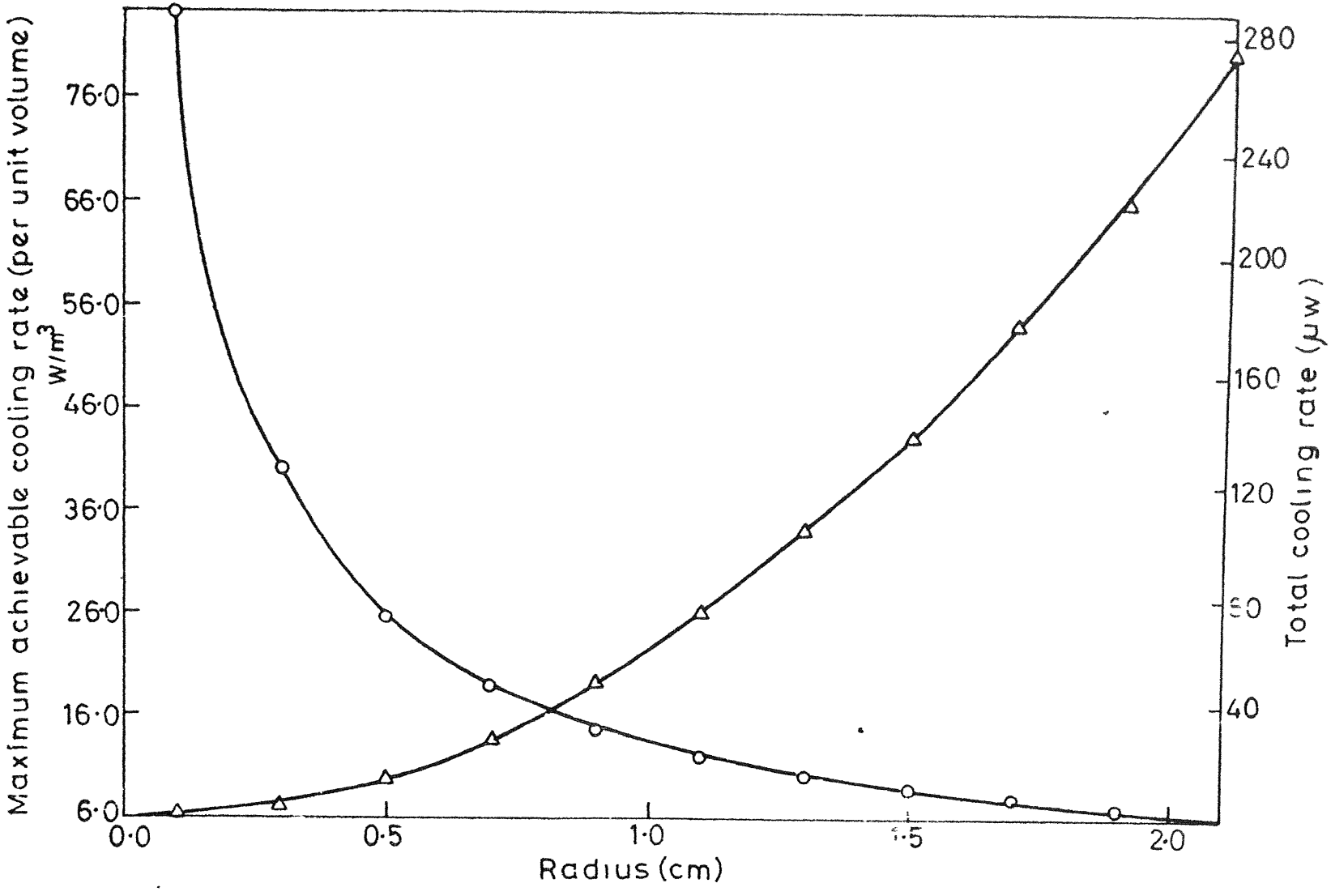

Fig 3·10 Maximum volumetric and total cooling rates for different tube radius

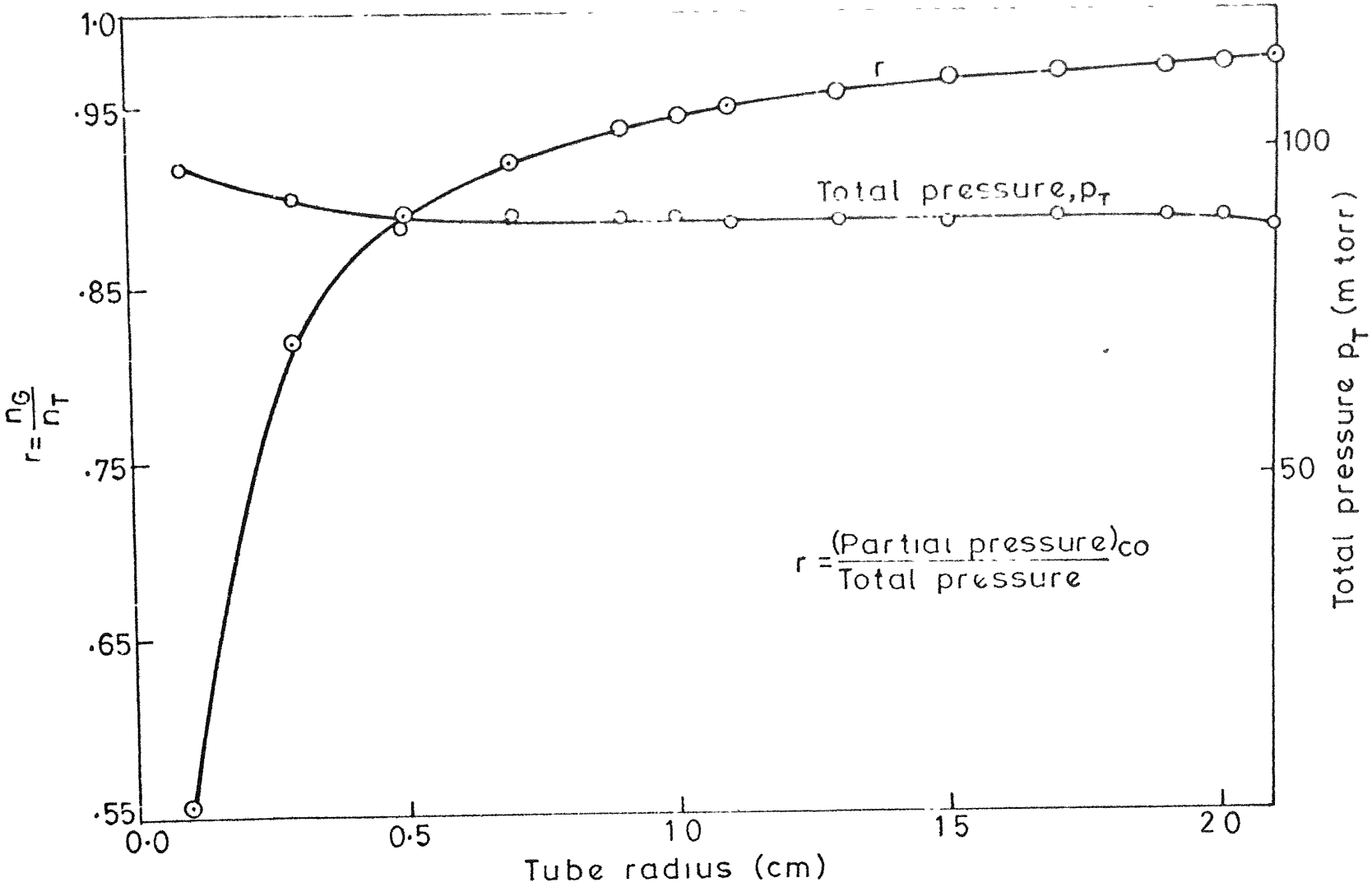

Fig.3·11 Total and partial pressures for achieving maximum cooling rates as a function of tube radius

Density of the ith species ($_i$) is evaluated using the ideal gas law :

$$i = \frac{n_i k}{R_i} \qquad (3.10)$$

where

k is Boltzman's constant = 1.38×10^{-23} J/°K,

R_i is the gas constant $[\frac{J}{kg\,^oK}]$ and $n_i(m^{-3})$ is the number of the ith species.

The gas constant (R) for CO is 296.9 $\frac{J}{kg\,^oK}$

and for CO_2 this value is 188.9 $\frac{J}{kg\,^oK}$

The specific heat (C_p) for CO is 1113 $\frac{J}{kg\,^oK}$

and for CO_2 it is 837 $\frac{J}{kg\,^oK}$ [13] .

Using the values of E_{Ri} listed in Table 3.2, the values of $u\Delta\theta_i$ can be calculated. Table 3.3 shows the maximum values of $(u\Delta\theta_i)$ achievable in the radiated zone for some tube radii. It can be easily seen that a flow speed of 0.1 m/s gives rise to a temperature drop which is 6.9°K for 0.1 cm tube radius and 13.5°K for 2 cm tube radius. The temperature drops for the remaining tube radii lie in between these two values. If larger temp. drops are desired, lower values of the flow speed can be used.

Table 3.3

Maximum values of $u\Delta\theta_1$ achievable in the radiated zone as a function of tube radius

S.No.	Tube radius (cm)	Maximum value of $u\Delta\theta_1$ $[\frac{m\ K}{s}]$
1.	0.1	0.69
2.	0.5	1.17
3.	1.0	1.29
4.	1.5	1.32
5.	2.0	1.35

CHAPTER 4

POST RADIATION ZONE

4.1 INTRODUCTION

In the following sections, we discuss the cooling (or heating) effect in the region succeeding the radiation zone. Fig. 4.1 shows the two zones namely the radiation zone and the post radiation zone. In the analysis we will assume the following :

(a) The number densities or partial pressures of molecules in different energy levels is uniform throughout the radiation zone. This assumption is justified because the laser beam is sufficiently intense leading to saturation in the entire region thereby giving rise to uniform number densities of molecules in level 1 and 2.

(b) The spatial diffusion of molecules of a particular energy state, due to gradients in x-direction in the number densities in the post radiation zone is negligible.

By virtue of assumption (a), we immediately know the inlet conditions to the post-radiation zone. Assumption (b) simplifies the balance equation to be written for the number densities in the elemental volume Adx shown in Fig. 4.1.

It may also be pointed out here that one does not know, a priori, whether there will be a temperature drop or rise in

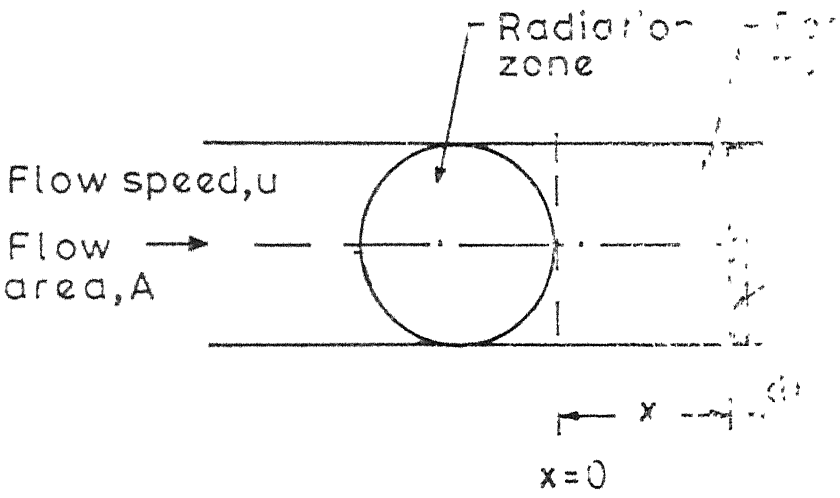

Fig. 4.1 Schematic representation and post radiation zone

the post-radiation zone. This is because whereas any trapping of the radiatively emitted radiation, as well as the collisional relaxation processes represented by k_{21} and k_{34} will lead to heating, the resonant energy transfer to level 3 and subsequent escape of radiation leads to cooling. Thus the overall effect can only be found by a formal analysis of the post-radiation zone, which differs from that for the radiation zone in following respects :

(a) In the post-radiation zone there is no pumping of molecules from level 1 to 2.

(b) The number densities are functions of x.

4.2 RATE EQUATIONS

We begin by defining the reference x = o, at the end of the radiation zone where the number densities n_i, i = 1 to 4 are known from calculations in Chapter 3. Although the end of this zone will be a curved surface, we will assume it to be a plane passing through the outer most point of the radiation zone. One may also consider x to be measured from the curved exit surface of the radiation zone.

Writing a balance equation for n_2, assuming that there is no accumulation of molecules in level 2 in the volume Adx, i.e., assuming steady state, we get :

$$Un_2(x) = un_2(x+dx) + (F_{21}A_{21}n_2+k_{23}n_2 - k_{32}n_3)dx \qquad (4.1)$$

... flow velocity u is taken to be uniform over the ... flow area A cancels out. Also k_{21} ... earlier. Similarly for level 3, we ...

$$n_3(x) \quad n_3(x+dx) + (\Gamma_{34}A_{34}n_3 + k_{32}n_3 - k_{23}n_2 + k_{34}n_4)dx \tag{4.2}$$

Eqns. (4.1) and (4.2) can be written in the form of following differential equations :

$$u\frac{dn_2}{dx} = -\Gamma_{21}A_{21}n_2 - k_{23}n_2 + k_{32}n_3 \tag{4.3}$$

and

$$u\frac{dn_3}{dx} = -\Gamma_{34}A_{34}n_3 + k_{23}n_2 - k_{32}n_3 - k_{34}n_4 \tag{4.4}$$

Introducing a new variable $\tau = \frac{x}{u}$, Eqn. (4.3) and (4.4) can be written as :

$$\frac{dn_2}{d\tau} = -\Gamma_{21}A_{21}n_2 - k_{23}n_2 + k_{32}n_3 \tag{4.3a}$$

$$\frac{dn_3}{d\tau} = -\Gamma_{34}A_{34}n_3 + k_{23}n_2 - k_{32}n_3 - k_{34}n_4 \tag{4.4a}$$

On substituting proper expressions for k_{ij}, we get

$$\frac{dn_2}{d\tau} = -\Gamma_{21}A_{21}n_2 - c_{23}n_4n_2 + c_{32}n_3n_1 \tag{4.5}$$

$$\frac{dn_3}{d\tau} = -\Gamma_{34}A_{34}n_3 + c_{23}n_4n_2 - c_{32}n_1n_3 - c_{34}n_4n_T \tag{4.6}$$

Eqns. (4.5) and (4.6) are two coupled differential equations and can be solved using the standard Runge-Cutta-Gill method [14], once the initial conditions are known.

4.3 INITIAL CONDITIONS

In Section 3, we have derived the operating conditions namely, n_2 and n_3 for various tube radii. These can easily be obtained from Table 3.2. In eqns. (4.5) and (4.6), the number densities are related through eqns. (2.19) to (2.21).

It becomes clear that for a given tube radius n_T and n_G have been fixed for optimal cooling. Therefore, for a given tube radius eqn. (4.5) and (4.6) are coupled differential equations in two variables, namely, n_2 and n_3.

4.4 INITIAL CONDITIONS

Since we have only 2 variables, we need to establish initial conditions only for these two. In the radiation zone, which can be represented by $x \leq o$, we have saturation condition viz. $n_2 = \frac{nG}{2}$. Therefore, for our purpose

$$n_{20} = n_2 \Big|_{\tau \leq o} = \frac{n_G}{2},$$

$$n_{30} = n_3 \Big|_{\tau \leq o} = n_3 \Big|_{x \leq o}$$

The values of n_{30} have been printed out from the computer program represented by the flow chart given in Fig. 3.5.

Table 4.1

Initial Conditions for Various Tube Radii

S.No.	Radius, R cm	$n_{20} \times 10^{-20} (m^{-3})$	$n_{30} \times 10^{-20} (m^{-3})$
1	0.1	8.8	1.13
2	0.3	12.7	0.46
3	0.5	13.3	0.29
4	0.7	13.5	0.22
5	0.9	13.6	0.17
6	1.0	13.7	0.16
7	1.1	13.7	0.14
8	1.3	13.8	0.12
9	1.5	13.8	0.11
10	1.7	13.8	0.09
11	1.9	13.8	0.085
12	2.0	13.8	0.08
13	2.1	13.8	0.07

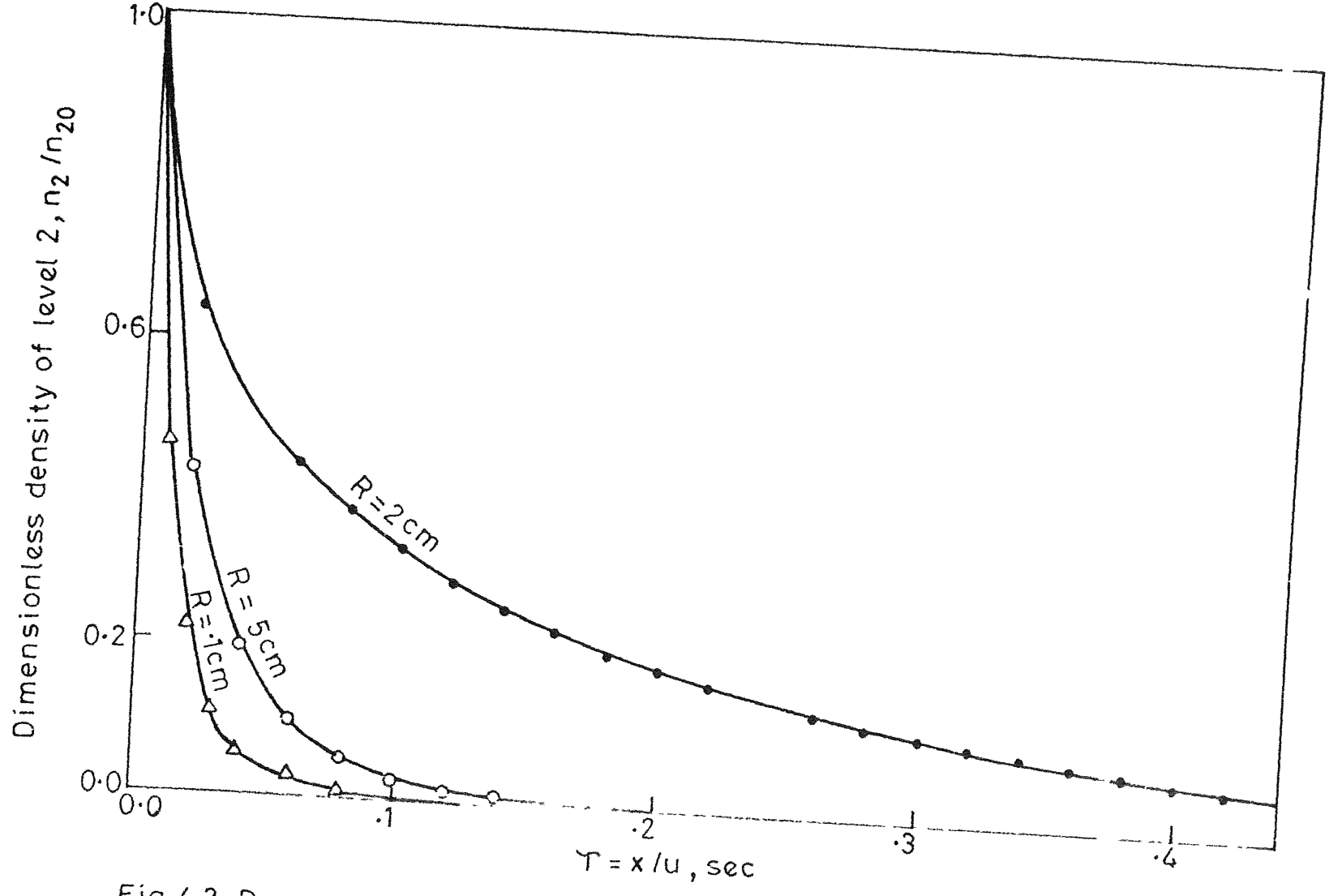

Fig 4 2 Dimensionless density of level 2 in the post radiation zone

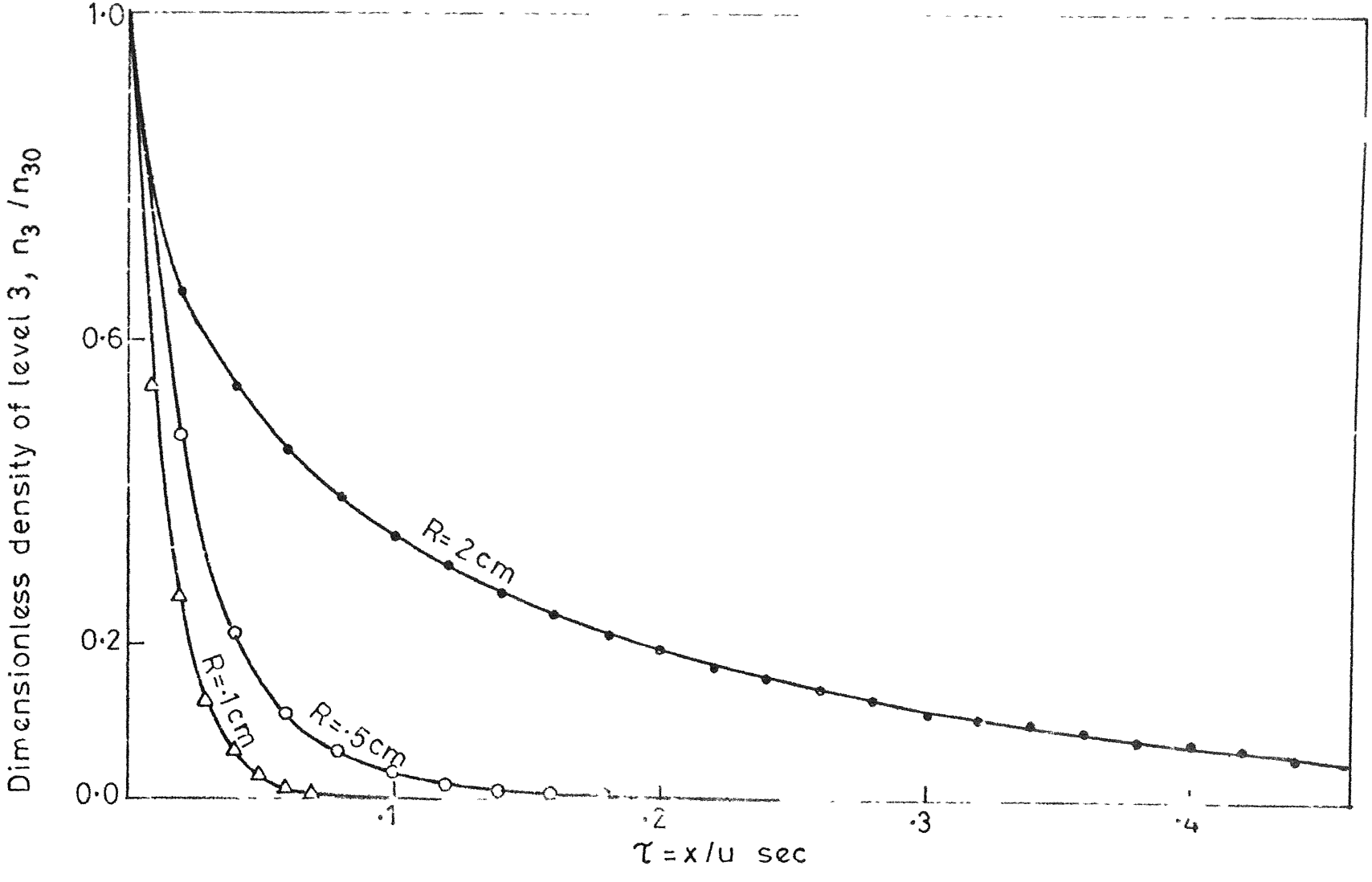

Fig.43 Dimensionless density of level 3 in the post radiation zone

Table 4.1 gives the values of n_{20} and n_{30} for various tube radii, corresponding to the optimum operating conditions.

By choosing an appropriate step size, the dimensionless number densities, i.e., n_2/n_{20} and n_3/n_{30} have been obtained as a function of τ using R-K-G method for all tube radii, and have been summarised for tube radii 0.1 cm, 0.5 cm and 2 cm in Figs. 4.2 and 4.3.

This exercise enables us to obtain the number densities as a function of τ which will be used in the next section for evaluating the cooling (or heating) effect in the post-radiation zone.

4.5 ENERGY REMOVAL RATE IN THE POST-RADIATION ZONE

As explained earlier in Chapter 2, the cooling or heating effect is brought about by a change in the translational energy of the gaseous mixture. For a system of $CO-CO_2$, the rate of change of translational energy per unit volume can be written as given in eq. (2.16). As has already been indicated, the term involving k_{21} is negligible for the $CO-CO_2$ system.

Hence, eqn. (2.16) can be written as :

$$\frac{dE_t}{dt} = n_3 k_{34}(E_3-E_4) - n_2 k_{23}(E_3-E_2) + n_3 k_{32}(E_3-E_2) \quad (4.7)$$

substituting proper expressions for k_{ij},

$$\frac{dE_t}{dt} = n_3 C_{34} n_I (E_3-E_4) - n_2 C_{23} n_4 (E_3-E_2) + n_3 C_{32} n_1 (E_3-E_2) \quad (4.8)$$

Here n_2 and n_3 are functions of τ. The cooling rate is the negative of the rate of change of translational energy. Eqn. (4.8) gives the rate of change of translational energy per unit volume at a given value of τ. Integrating eqn. (4.8) over the entire volume of the post-radiation zone, we can get the total rate of increase in the translational energy in this zone. Denoting the negative of this quantity by E_{R2}, we have

$$E_{R2} = -\int_o^\infty \frac{dE_t}{dt} A\, dx$$

$$= -uA \int_o^{\tau_{max}} (\frac{dE_t}{dt}) d\tau \qquad (4.9)$$

$$= uA\, I_n \qquad (4.9a)$$

where

$I_n = -\int_o^{\tau_{max}} (\frac{dE_t}{dt})\, d\tau$, and τ_{max} has been chosen such that n_2 and n_3 have almost dropped to zero values at $\tau = \tau_{max}$.

Once n_2 and n_3 have been calculated as functions of , as represented in Figs. 4.2 and 4.3 for representative tube radii, the values of I_n can be calculated by Simpson's rule using eqn. (4.8), together with the initial conditions given in Table 4.1. These values of I_n are listed in Table 4.2. It is seen that I_n is positive, which means that there will be a temp. drop in the post-radiation zone. This is calculated in the next section.

4.6 TEMPERATURE DROP IN POST-RADIATION ZONE

Temperature drop $\Delta\Theta_2$ in the post-radiation zone can now be easily calculated by a simple energy balance :

$$[(\rho C_p)_{co} + (\rho C_p)_{co_2}]\ uA\ \Delta\Theta_2 = E_{R2},$$

or

$$\Delta\Theta_2 = \frac{I_n}{[(\rho C_p)_{co} + (\rho C_p)_{co_2}]} \qquad (4.10)$$

Using the values of ρC_p given in Chapter 3, $\Delta\Theta_2$ has been calculated, and is tabulated in Table 4.2, as a function of tube radius at the optimum operating conditions.

It is seen that there is a temp. drop of the order of 2 to 3K in the post-radiation zone, which can be added to the temp. drop, $\Delta\Theta_1$ in the radiation zone. It may be pointed out that $\Delta\Theta_2$ is independent of the flow velocity, whereas $\Delta\Theta_1$ is inversely proportional to the flow velocity (see Table 3.3).

Table 4.2

Temperature Drop in the Post-Radiation Zone

Tube Radius (cm)	Integral I_n (J/m^3)	$\Delta\Theta_2$(K)
0.1	0.47	2.0
0.3	0.49	2.92
0.5	0.38	2.54
0.7	0.36	2.34
0.9	0.37	2.45
1.0	0.38	2.5
1.1	0.39	2.57
1.3	0.40	2.66
1.5	0.40	2.74
1.7	0.42	2.82
1.9	0.43	2.89
2.0	0.43	2.90
2.1	0.43	2.90

Equation (5.1) can also be rewritten as

$$\frac{n_1}{n_2} = \frac{W_{21}}{W_{12}} + \frac{(A_{21}+k_{21}+k_{23})(A_{34}+k_{32}+k_{34}) - k_{32}k_{23}}{W_{12}(A_{34}+k_{32}+k_{34})} \qquad (5.2)$$

For saturation n_1 should be equal to n_2. In the expression given above the first term is equal to one because W_{12} is equa. to W_{21}. Therefore, to make n_1 equal to n_2,, the second expression on the right hand side of E_9eqn. (5.2) should be made negligible as compared to 1. This is achieved by making the denominator sufficiently larger in comparison to the numerator. This condition is achieved when

$$W_{12}(A_{34}+k_{32}+k_{34}) \backsim 10(A_{21}+k_{21}+k_{23})(A_{34}+k_{32}+k_{34})-10k_{32}k_{23} \qquad (5.3)$$

Neglecting k_{21} for reasons explained in Section 3.8, and substituting proper expressions for rate constants, the condition for saturation is given as

$$W_{12} = 10(A_{21}+C_{23}n_4) - \frac{10C_{32}C_{23}n_1n_4}{A_{34}+C_{32}n_1+C_{34}n_T} \qquad (5.4)$$

The most conservative estimate for laser power calculation is the one when levels 2 and 3 are assumed to be empty. Physically this situation occurs only at the beginning. This fact further justifies dropping of the radiative trapping terms. At the beginning, since levels 2 and 3 are almost empty, F_{21} and F_{34} are equal to 1, leaving A_{21} and A_{34} unaltered.

With this simplification, n_4 could be replaced by n_H and n_1 by n_G. Further, n_G is equal to r times n_T and n_H is equal to $(1-r)n_T$. With these modifications, the saturation condition becomes :

$$W_{12} = 10(A_{21}+C_{23}(1-r)n_T) - \frac{10(C_{32}C_{23})(r)(1-r)n_T^2}{A_{34}+(rC_{32}+(1-r)C_{34})n_T} \qquad (5.5)$$

In eqn. (5.5) if r and n_T are known, W_{12} can be determined using the other constants that have been derived in Sections 2.4 and 2.5. The values of r and n_T are the operating ones which have been derived in Chapter 3 for various tube radii and summarised in Table 3.2.

The intensity of the laser beam required is given by the expression [15]

$$I = \frac{W_{12}[E_2-E_1]n_1}{K\, g_o\, n_1} \qquad (5.6)$$

where k is given by

$$K = \frac{\lambda_{21}^2 A_{21}}{8\pi} \qquad (5.7)$$

if the multiplicities of levels 1 and 2 are assumed to be the same. For CO gas, corresponding to levels in Fig. 2.1, $\frac{1}{\lambda_{21}} = 2143$ cm and $A_{21} = 33.8$ sec^{-1} which gives us

$$K = 2.928\times10^{-11} \quad m^2\ sec^{-1}$$

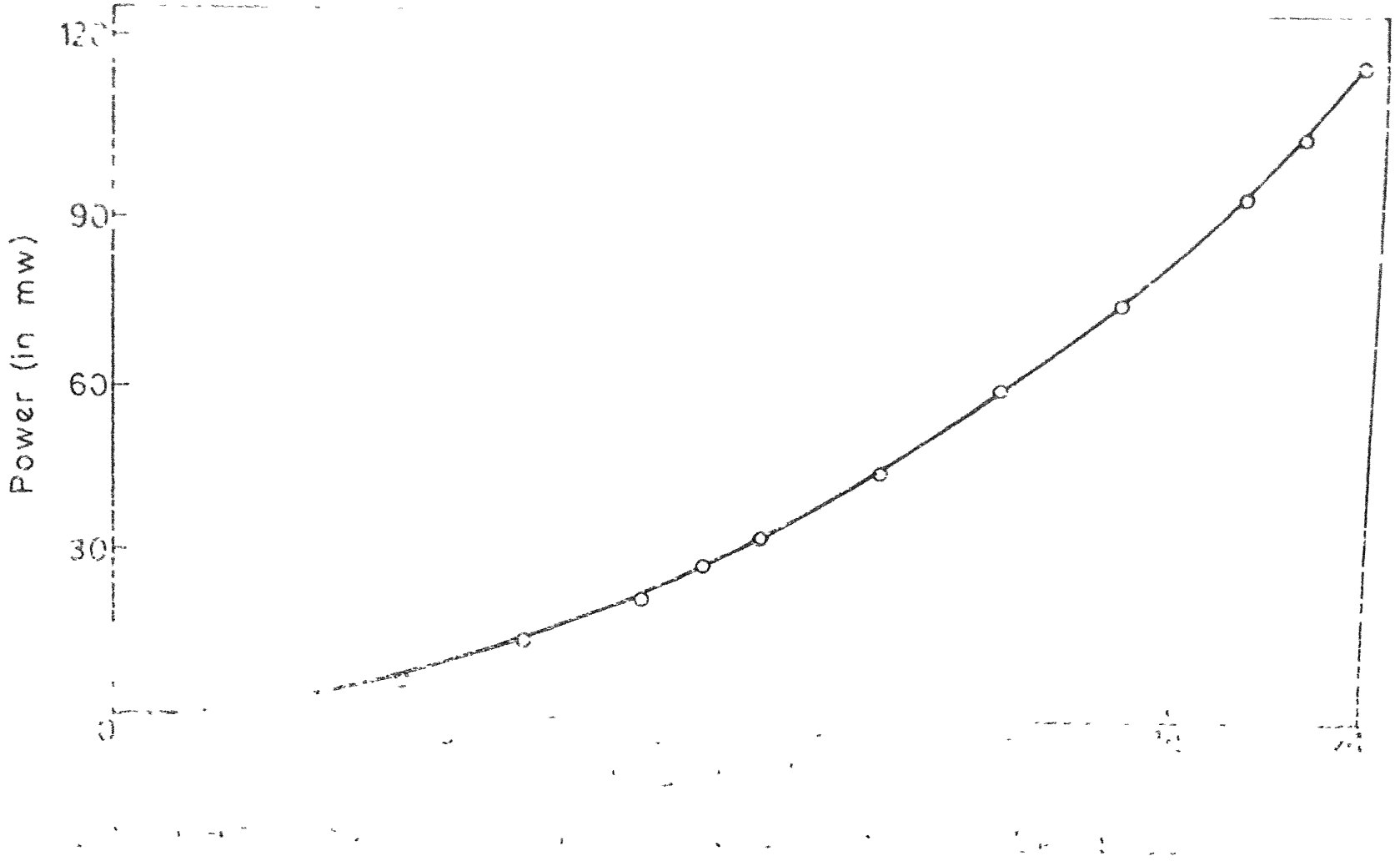
Power (in mw)
90
60
30
0

g_o, which is the line shape function, is given by

$$g_o = \frac{.939}{\Delta\nu_D} \qquad (5.8)$$

for the case of Doppler broadening.

$\Delta\nu_D$ has been explained in Section 2.7 and for CO gas, the value has been computed as 1.507×10^8 Hz.

All these values put together in eqn. (5.6) gives us the intensity I is multiplied with the area of cross section of the beam, which is the same as that of the tube through which the gas flows. The results of the calculations are shown in Fig. 5.1.

5.3 COMPARISON WITH CONVENTIONAL SYSTEM

In this section, the proposed system is compared with a conventional system operating at similar conditions of total pressure, partial pressures, flow speed and tube radius. We evaluate the temperature difference required across the tube wall, for the same amount of heat removal rate as for the proposed one.

For this calculation, we assume that the convective film at the outer surface of the wall and tube wall, do not provide any resistance to heat flow. The resistance to heat flow therefore may be calculated on the basis of the convective film on the inner side of the tube only.

We first check whether the flow is laminar or turbulent, to decide on the appropriate correlation to be used for evaluating the heat transfer coefficient. For this purpose we evaluate the Reynolds number, given as :

$$R_e = \frac{uD\rho}{\mu}$$

where

u is the flow speed (m/s),

D is the diameter of the tube in which the flow occurs (m)

and μ is the viscosity of the gas flowing (kg $m^{-1}s^{-1}$)

The viscosity is evaluated using the expression [ ] :

$$\mu = 2.669 \times 10^{-6} \frac{\sqrt{MT}}{\sigma^2 \Omega_\mu} \qquad (5.9)$$

where

M is the molecular weight of the gas,

T is the absolute temperature (K),

σ is the characteristic diameter of the molecule (A^o),

and Ω_μ is a slowly varying function of the dimensionless temperature $\frac{kT}{\epsilon}$. Both k/ϵ and Ω_μ are tabulated functions.

Equation (5.9) is found to be applicable to monoatomic as well as polyatomic gases [13].

For CO at $T = 300^{o}K$

$$\sigma = 3.59 \text{ Å}$$

and $$\Omega_{\mu} = 1.064$$

which for $M = 28$ gives

$$\mu = 1.78 \times 10^{-5} \quad m^{-1} s^{-1}$$

For CO_2 at $T = 300^{o}K$

$$\sigma = 3.996 \text{ (Å)}$$

and $$\Omega_{\mu} = 1.283$$

which for $M = 44$ gives

$$\mu = 1.5 \times 10^{-5} \quad m^{1} s^{-1}$$

The viscosity for a mixture of gases is evaluated using [13] :

$$\mu_{mix} = \sum_{i}^{n} \frac{x_i \mu_i}{\sum_{j}^{n} x_j \Phi_{ij}} \tag{5.10}$$

in which

$$\Phi_{ij} = \frac{1}{\sqrt{8}} \left(1+ \frac{M_i}{M_j}\right)^{-1/2} \left[1+\left(\frac{\mu_i}{\mu_j}\right)^{1/2} \left(\frac{M_j}{M_i}\right)^{1/4}\right]^2 \tag{5.11}$$

where

n is the number of chemical species in the mixture,

x_i and x_j are the mole fractions of species i and j,

μ_i and μ_j are the viscosities of species i and j at the system temperature and pressure

and M_i and M_j are the corresponding molecular weights.

Since in our case, the viscosity for CO and CO_2 are of the same order and the mole fraction of CO_2 is very small, we could approximate μ_{mix} by μ_{co}. Using this approximation, and a flow speed of 0.1 m/s for a tube radius 1 cm,

$$R_e \sim 0.015 \quad ,$$

in which the density (ρ) has been evaluated using :

$$\rho = \rho_{co} + \rho_{co2} \tag{5.12}$$

ρ_{co} and ρ_{co2} are calculated using eqn. (3.10) and for this particular case, their values are :

$$\rho_{co} = 126.6 \times 10^{-6} \quad kg/m^3$$

and

$$\rho_{co2} = 11.6 \times 10^{-6} \quad kg/m^3$$

The Reynolds number for other tube radii will also be of the same order. For a flow through a duct, this value of Reynold number indicates that the flow is laminar. We can now use an appropriate relationship to find the heat transfer coefficient.

For a fully developed laminar flow through a duct

$$N_u = 4.364 \tag{5.13}$$

for a constant wall heat flux [1]. N_u, the Nusselts number is given by

$$N_u = \frac{hD}{k}$$

where

h is the heat transfer coefficient (W/m^2 K),

k is the thermal conductivity of the gas (W/mK)

and D is the diameter of the tube (m).

The thermal conductivity k is calculated using [13],

$$k = (C_p + \frac{5}{4}\frac{R}{M})\mu \qquad (5.14)$$

where

C_p is the specific heat of the gas (J/kg K),

R is the universal gas constant and has a value of 8314 (J/kg.mole K),

M is the molecular weight,

and μ is the viscosity of the flowing gas (kg m^{-1} s^{-1}) .

For CO,

$$M = 28,$$

$$C_p = 296.9\ (\frac{J}{kg\ K})$$

and

$$\mu = 1.78 \times 10^{-5}\ \frac{kg}{mK}$$

which gives

$$k_{co} = 0.026\ \frac{W}{mK}$$

and for CO_2,

$$M = 48$$

$$C_p = 188.9(\frac{J}{kg^oK})$$

and $\mu = 1.5 \times 10^{-5} \ \frac{kg}{mK}$

which gives

$$k_{co} = 0.0161 (W/mK)$$

The thermal conductivities of gas mixtures at low density may be estimated by a method analogous to that previously given for viscosity (eqn. (5.10)) [13] :

$$k_{mix} = \sum_{i=1}^{n} \frac{x_i k_i}{\sum_{j=1}^{n} x_j \Phi_{ij}} \qquad (5.15)$$

The terms in the expression given above have the same meaning as for eqn. (5.10).

Since the values of thermal conductivity k, for CO and CO_2 are almost of the same magnitude, one could use,

$$k_{mix} \backsim 0.024 \ \frac{W}{mK}$$

Using this value of k, we can write

$$hD = 0.1047 \qquad (5.16)$$

using eqn. (5.13)

The temperature difference ΔT, required to be maintained across the tube wall for effecting a heat removal rate, E_{R1}, can be calculated using the expression

$$E_{R1} = hS_A \Delta T \qquad (5.17)$$

where

S_A is the surface area across which heat flow occurs (m^2) .

Surface area S_A for a tube of diameter D and length L is πDL. Using L $\sim$ D, as in the proposed laser induced cooling scheme, ΔT can be calculated for the various values of E_{R1} given in Table 3.2. For example, for R = 1 cm, we get

$$h \sim 5 W/m^2K$$

and

$$T \sim 10^{-2}K.$$

Thus we see that the temperature differential required between the coolant and the fluid stream to be cooled is indeed very small for removing the quantities of heat that a laser induced cooling system removes.

However, the value of heat transfer coefficient obtained through eqn. (5.13) appears to be unrealistic for this case. This needs to be improved upon. Perhaps eqn. (5.13) is not applicable for flow of gases through a duct at pressures of the order of 100 mtorr, as is the case here, especially when the duct diameters are also of the order of 10^{-2} m or so.

This comparison was made on the basis of heat removal rates. It should, however, be noted that in laser induced cooling system, one can achieve higher temperature drops over very small axial distances by reducing the flow speed. Such large temperature drops over a small distance cannot possibly be achieved in a conventional system.

CHAPTER 6

CONCLUSIONS AND SUGGESTIONS

In this work, steady state cooling of a mixture of CO and CO_2, using laser radiation has been considered. The mixture flows in a tube and the laser beam falls perpendicular to it. The optimal operating conditions (partial pressures of the constituent gases) for maximum cooling have been obtained for several tube radii. These, together with the cooling rates are listed in Table 3.2. Although cooling will take place of if the total pressure is less than 200 mtorr[ ], optimal operating pressures are in the range of 90 - 100 mtorr for tube radii ranging from .1 cm to 2 cm. The maximum volumetric cooling rates achieved are in the range of 6 W/m^3 to 90 W/m^3, and are higher for low tube radii.

The important effect that has been included is the radiation trapping. It is because of this phenomenon that cooling rates are high for low tube radii. With an increase in the tube radius, the cooling rates come down significantly. However, for larger radii, the volume integrated cooling rates are larger. For a tube of diameter 1 cm, the volumetric cooling rate is 25.8 W/m^3 and the volume integrated cooling rate is 14.5 μW. These values are obtained for a total pressure of 92.7 mtorr and a partial pressure of CO 82.6 mtorr. A temperature drop of

12^{o} can be achieved with a flow speed 0.1 m/s in a tube of diameter 1 cm.

In this work, analysis has been done for flow in a tube with a circular cross section illuminated by a laser beam which is also circular in cross section. Analysis for rectangular and other sections of tube as well as laser beam could be done on similar lines. Further, the total cooling rate per unit laser power could be maximised and optimal operating conditions determined. The dependence of the rate constants on temperature could also be accounted for.

REFERENCES

[1] E.R.G. Eckert and R.H. Drake, in : Analysis of Heat and Mass Transfer, (McGraw Hill Inc., 1972).

[2] T.W. Hansch and A.L. Schawlow, Optics Comm. 13 (1975) 68.

[3] A. Ashken, Phys. Rev. Lett 40 (1978) 729.

[4] P.R. Berman and S. Stenholm, Optics Comm. 24 (1979) 155.

[5] N. Djeu, Optics Comm. 26 (1978) 354.

[6] J.S. Goela and R.K. Thareja, Optics Comm. 40 (1982) 254.

[7] J.S. Goela and R.K. Thareja, Optics Comm. 42 (1982) 418.

[8] W.H. Christiansen and A. Hertzberg, Proc. IEEE 61 (1973) 1060.

[9] T.A. Cool, in : Handbook of Chemical Lasers, eds. R.W.F. Gross and J.F. Bott (John Wiley and Sons, N.Y. 1976).

[10] P.K. Cheo, in : Lasers, vol. 3, eds. A.K. Levine and A.J. De maria (Marcel Dekker Inc., N.Y. 1971).

[11] T. Holstein, Phys. Review 72 (1947) 1212.

[12] S.S. Rao : Optimization theory and application (Wiley Eastern Limited, 1978).

[13] R.B. Bird, W.E. Stewart and E.N. Lightfoot Transport Phenomenon (John Wiley and Sons, N.Y. 1960).

[14] A. Ralston and H.S. Wilf : Mathematical Methods for Digital Computers, vol. 2 (John Wiley and Sons, N.Y. 1961).

[15] B.A. Lengyle, Introduction to laser physics (John Wiley and Sons, N.Y. 1966).

ME-1984-M-JAI-LAS